

THE CONCEPT OF THE PSEUDOSPINODAL
IN CRITICAL PHENOMENA

by

JUNAIDAH OSMAN

B.S., Northern Illinois University, 1978

A MASTER'S THESIS


submitted in partial fulfillment
of the requirements for the degree

MASTER OF SCIENCE

Department of Physics
KANSAS STATE UNIVERSITY
Manhattan, Kansas

1981

Approved by:


Major Professor

**THIS BOOK
CONTAINS
NUMEROUS PAGES
WITH THE ORIGINAL
PRINTING BEING
SKEWED
DIFFERENTLY FROM
THE TOP OF THE
PAGE TO THE
BOTTOM.**

**THIS IS AS RECEIVED
FROM THE
CUSTOMER.**

**THIS BOOK
CONTAINS
NUMEROUS PAGES
WITH ILLEGIBLE
PAGE NUMBERS
THAT ARE CUT OFF,
MISSING OR OF POOR
QUALITY TEXT.**

**THIS IS AS RECEIVED
FROM THE
CUSTOMER.**

SPEC
COLL
LD
2668
T4
1981
D85
C.2

TABLE OF CONTENTS

LIST OF FIGURES	iv
LIST OF TABLES.	v
ACKNOWLEDGEMENTS.	vi
Chapter	
1. INTRODUCTION	1
2. BASIC CONCEPTS OF CRITICAL PHENOMENA	16
A. Order Parameter and Order of Phase Transitions	16
B. Choice of Variables.	20
C. Critical-Point Exponents and Power Laws.	26
D. Generalized Homogeneous Functions and the Homogeneity Postulate.	33
E. Scaling Laws for Equation of State and Thermodynamic Functions.	37
F. Universality	39
3. DERIVATION OF THE EQUATION OF STATE FROM THE PSEUDO- SPINODAL ASSUMPTION.	41
A. The Spherical Model.	42
B. Derivation of $h(x)$ from the Revised Pseudospinodal Assumption	45
C. Universal Amplitude Ratios: Γ/Γ' , ξ_0/ξ_0' and R_x	47
D. Derivation of A/A'	49
4. NUMERICAL CALCULATION AND RESULTS.	53
A. Numerical Calculations	53

B. Results.	55
C. Analyticity of Equation of State	70
5. EVIDENCE FOR THE UNIVERSALITY OF THE PSEUDOSPINODAL.	77
6. CONCLUSION	90
REFERENCES.	93
APPENDIX A.	96
ABSTRACT	

LIST OF FIGURES

Figure		Page
1.	A Plot of Mean Pressure Versus Volume for One Mole of van der Waal's Fluid	3
2.	Measurements on Eight Fluids of the Coexistence Curve.	8
3.	Typical Solid-liquid-gas and Ferromagnetic Phase Diagrams.	17
4.	Coexistence Curve of Argon in Terms of Two Sets of Variables.	22
5.	P(V) Isotherms and $\mu(\rho)$ Isotherms of Argon in the Critical Region	24
6.	Critical Exponents for Power-law Anamolies of Thermodynamic Properties	29
7.	Percent Deviation Plot of Our Equation of State from the Equation of Milosëvić and Stanley for the (3,3) Model System	68
8.	Percent Deviation Plot of Our Equation of State from the Equation of Gaunt and Domb for the (3,1) Model System.	71
9.	Comparison of Our Equation of State to the Equation of Gaunt and Domb for the (2,1) Model System.	73
10.	Plot of Pseudospinodal Curve Data $ \Delta\rho_S^* $ Normalized by the Coexistence Curve $B_C\Delta T^*$ versus ΔT^*	87

LIST OF TABLES

Table	Page
1. A Comparison between Typical Experimental Results and the Classical Results on the Behavior of Magnetic and Liquid-gas Systems Near the Critical Point	11
2. Values of Critical-point Exponents for Selected Systems. . .	31
3. (3,1) Model System: Values of Γ/Γ' , R , and ϵ_0/ϵ_0' Obtained Using Several Different Values of C	56
4. (3,2) Model System: Values of Γ/Γ' and R Obtained Using Several Different Values of C	57
5. (3,3) Model System: Values of Γ/Γ' and R Obtained Using Several Different Values of C	58
6. (2,1) Model System: Values of Γ/Γ' and R Obtained Using Several Different Values of C	59
7. (3,1) Model: Comparison of Universal Amplitude Ratios . . .	62
8. (3,2) Model: Comparison of Universal Amplitude Ratios . . .	63
9. (3,3) Model: Comparison of Universal Amplitude Ratios . . .	64
10. (2,1) Model: Comparison of Universal Amplitude Ratios . . .	65
11. Specific Heat of He^4 : Results of Fitting the Data Along Each Isochore to $C_V^*/T = A(\Delta T^* + \Delta T_S^*)^{-\alpha}$	80
12. Specific Heat of CO_2 : Results of Fitting the Data Along Each Isochore to $C_V^*/T = A(\Delta T^* + \Delta T_S^*)^{-\alpha}$	81
13. Thermal Conductivity of CO_2 : Results of Fitting the Data Along Each Isochore to $\lambda = \lambda_0(\Delta T^* + \Delta T_S^*)^{-\kappa}$	82
14. Inverse Isothermal Compressibility of He^4 : Results of Fitting the Data Along Each Isochore to $(K_T^* \rho^{*2})^{-1} = 1/r(\Delta T^* + \Delta T_S^*)^\gamma$	83
15. A List of Pseudospinodal and Coexistence Curves.	84

ACKNOWLEDGMENT

I dedicate this work to my late father who had given me, throughout his life, a lot of encouragement to pursue higher education.

I am deeply indebted to my major professor, Dr. Chris Sorensen, for the patience, understanding and invaluable guidance he has given me throughout the course of this project.

I also acknowledge the financial support of the University of Science Malaysia that has made my study here possible.

To the faculty and staff of the Physics Department and my fellow graduate students, I wish to express my sincere thanks for their friendliness which has made my stay here enjoyable and memorable.

To my husband Sani and family back home, I thank them all for their continued moral support.

Chapter 1

INTRODUCTION

The study of critical phenomena deals with the behavior of a system near its critical point. This is the point where the phase transition line of a system terminates, that is, where distinction between phases (for example liquid and vapor phases) disappear. A wide variety of physical systems in nature exhibit anomalous behavior near their critical points. Liquid-gas systems, binary fluids, ferromagnets and magnetic alloys are all known to behave oddly. It has been found that thermodynamic properties of these systems diverge as the critical point is approached. The specific heat of a gas for example diverges. The isothermal susceptibility of a ferromagnet grows very rapidly in the region of its Curie temperature. It has also been observed in light-scattering experiments that a fluid scatters light strongly due to very strong density fluctuations, at the critical point.

The attempts to predict, explain, or even describe these behaviors at the critical point have met with varying degrees of success. One of the earliest attempts was the theoretical work of van der Waals in 1873. The van der Waals theory now represents one of the classical theories in critical phenomena. It has now become customary to divide all the existing theories of critical phenomena into two categories: the classical theories and the present or modern theories of critical phenomena.

In this introductory section, the classical theories will be reviewed so as to provide a historical perspective of critical phenomena

and also to give us a better qualitative understanding of the subject. The modern theories will be mentioned briefly before we introduce the main subject of this thesis.

A. The Classical Theories:

The ideal gas law,

$$PV = NkT = nRT \quad (1)$$

is the simplest theory of a fluid system which assumes that gas particles interact very weakly with one another so that these interactions can be neglected altogether.

In Eq. (1), P and V are pressure and volume of the fluid respectively, $n = N/N_A$ is the number of moles of gas in the system, N_A is the Avogadro number, k is the Boltzmann constant and R is the ideal gas constant. For a gas at low densities and at high pressures, this equation is fairly well obeyed. To describe a gas at normal densities, van der Waals introduced the notion of imperfect or non-ideal gas. According to the van der Waals theory, an approximate equation of state of a fluid system is given by

$$P = \frac{RT}{(\bar{V} - b)} - \frac{a}{\bar{V}^2} \quad (2)$$

where $\bar{V} = V/n$ is the volume per mole, a and b are phenomenological parameters characteristic of the fluid. The theory assumes that gas molecules have finite volume which means there is a limit to the volume V in Eq. (1). This is represented by the excluded volume term b in Eq. (2). It further assumes that there exists an attractive force between the gas molecules which leads to a decrease in pressure represented by the term a/\bar{V}^2 in Eq. (2).

Figure 1 shows the behavior of one mole of van der Waals' fluid

**THIS BOOK
CONTAINS
NUMEROUS PAGES
THAT WERE
BOUND WITHOUT
PAGE NUMBERS.**

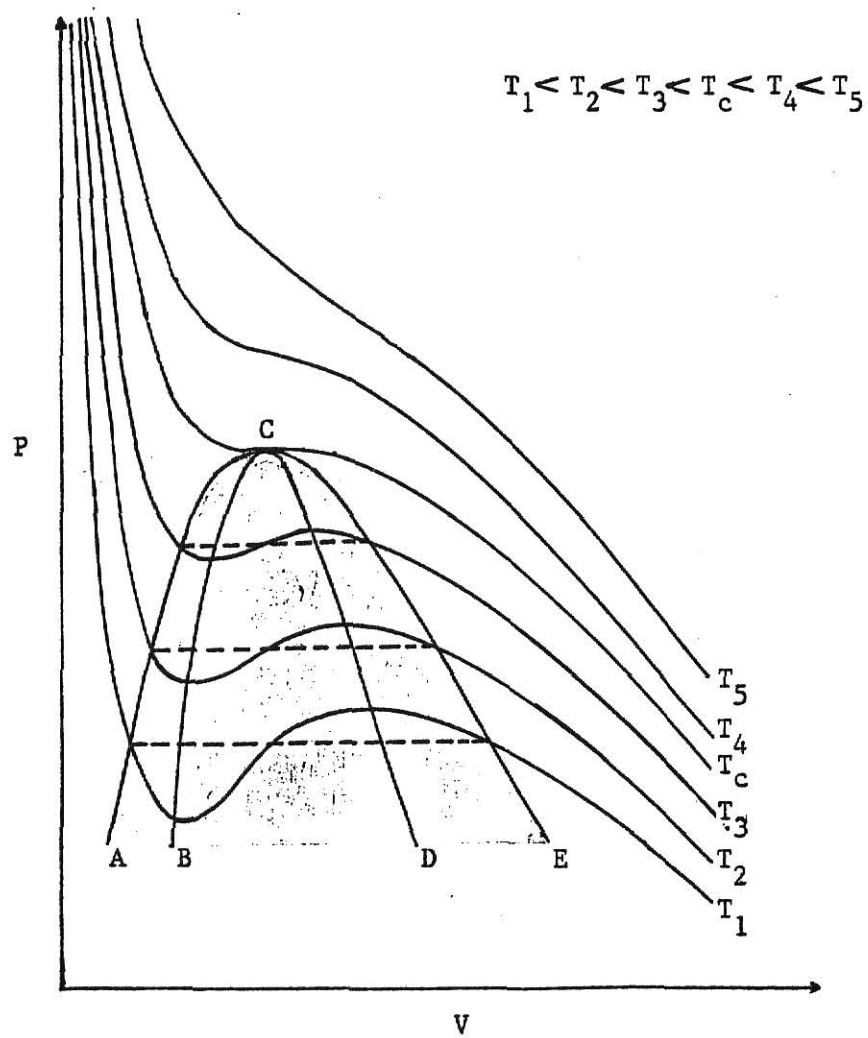
**THIS IS AS
RECEIVED FROM
CUSTOMER.**

FIGURE 1

A schematic plot of mean pressure versus volume for one mole of van der Waals' fluid at various temperatures T using Eq. (2).

**THIS BOOK
CONTAINS
NUMEROUS PAGES
WITH DIAGRAMS
THAT ARE CROOKED
COMPARED TO THE
REST OF THE
INFORMATION ON
THE PAGE.**

**THIS IS AS
RECEIVED FROM
CUSTOMER.**



when a graph of mean pressure is plotted against volume at various temperature T using Eq. (2). At high temperatures, the fluid has only one unique volume V and thus only one phase exists, namely the gas phase. In this high temperature region, the behavior of the gas can be approximately described by the ideal gas law, which is clearly demonstrated by Eq. (2) if we let a and b become negligible. The pressure is a monotonic decreasing function of volume so that the isothermal compressibility $K_T = -\frac{1}{V} (\partial V / \partial P)$ is positive and finite at high temperatures. As the temperature T decreases to the value T_c , there is a horizontal inflection point C on the P - V isotherm. At this point, the slope $(\partial P / \partial V) = 0$ and $(\partial^2 P / \partial V^2) = 0$; thus the isothermal compressibility is infinite. The point C is called the critical point of the fluid and T_c is the critical temperature. Below the critical temperature all isotherms exhibit a "loop." At these temperatures, below T_c , the van der Waals fluid acquires three different values of volume V for each value of pressure P . However, one of the values is unphysical since it lies in the region between the maximum and the minimum where the slope $\partial P / \partial V$ is positive implying a negative isothermal compressibility. The fluid then co-exists in two different phases, namely the liquid and gas phase. The Maxwell equal area construction, which replaces the loops by straight lines represented by the broken straight lines in Figure 1, ensures that the liquid and the gas phase have the same chemical potential, temperature and pressure; thus ensures that the two phases co-exist in equilibrium. The two-phase region represented by the shaded region in Figure 1 is bounded by the curve ACE called the coexistence curve. The maxima and the minima are bounded by the curve BCD which is called the spinodal curve. The region between these two curves is the metastable state of

the van der Waals fluid (superheated liquid, supersaturated gas).

Using the conditions $\partial P / \partial V = 0$ and $\partial^2 P / \partial V^2 = 0$, we can show that at the critical point

$$V_c = 3Nb, \quad P_c = \frac{1}{27} \frac{a}{b^2}, \quad RT_c = \frac{8a}{27b}. \quad (3)$$

With these values we can eliminate the parameters a and b in Eq. (2) to obtain

$$\left(\tilde{P} + \frac{3}{\tilde{V}^2} \right) (3\tilde{V} - 1) = 8\tilde{T} \quad (4)$$

where $\tilde{P} = P/P_c$, $\tilde{V} = V/V_c$ and $\tilde{T} = T/T_c$. This new form of van der Waals' equation means that if we measure pressure, volume and temperature, respectively, in units of P_c , V_c and T_c , then the equation of state is the same for all substances. Thus any two fluids with the same values of \tilde{P} , \tilde{V} and \tilde{T} may be said to be in corresponding states. This law of corresponding states together with the existence of the critical point demonstrated by the van der Waals theory suggest that the critical point is a general phenomena which exists in all gases.

The fact that magnetic systems also exhibit critical phenomena was discovered much later. The first theory to explain magnetic phase transition and the existence of the Curie temperature T_c was provided by Pierre Weiss in 1907. The now classical Weiss theory is greatly similar to the van der Waals theory for liquid-gas phase transition. Both of these classical theories assume that the attractive forces between the molecules which produce cooperative effects have a very long range. For this reason, they are also known as the mean-field theories. As a result, they both give the same quantitative description of critical phenomena. We shall simply quote their results here. The derivations are given in several books^{1,2} on critical phenomena.

a. At the critical point both theories predict

that the shape of the coexistence curve is quadratic. That is, for the van der Waals theory, the coexistence curve is given by

$$(\rho_L - \rho_G) \approx |T - T_c|^{1/2}$$

where ρ_L and ρ_G are liquid and gas densities respectively. And, for the Weiss theory,

$$M \approx |T - T_c|^{1/2}$$

where M is the magnetization of the magnet system.

b. At the critical point the specific heat displays a discontinuity.

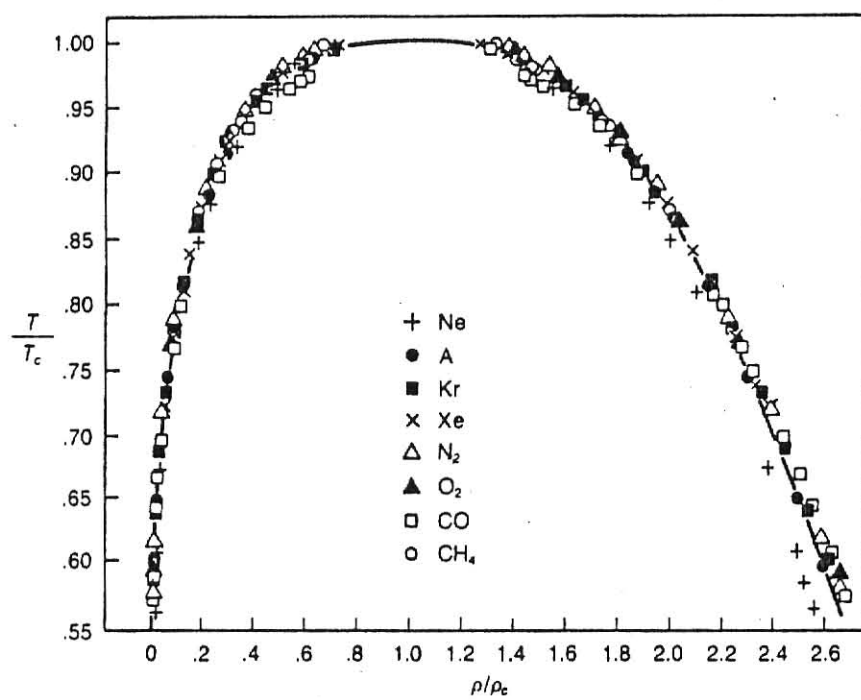
c. The compressibility or the susceptibility become infinite at the critical point as

$$1/(T - T_c).$$

Although the classical theories provide a correct qualitative description of critical phenomena their quantitative results quoted above disagree with almost all experiments. In the 1940's Guggenheim realized that the coexistence curve of a fluid system is not parabolic. The now classic Guggenheim plot is reproduced in Figure 2 which shows the temperature dependence of the liquid-gas density difference ($\rho_L - \rho_G$) for eight different simple fluids. The fact that the data, properly normalized, fall on one and the same curve is in accord with the law of corresponding states. The shape of the solid curve is a cubic function rather than the quadratic function that the classical theories would predict. Experiments done on specific heat of fluid and magnetic systems show that the specific heat of these systems diverges at the critical point according to a certain power law which disagrees completely with

FIGURE 2

Measurements on eight fluids of the coexistence curve. The solid curve corresponds to a fit to a cubic equation. From Ref. 44.



the classical results. The compressibility and the susceptibility are found to diverge more strongly at the critical point than the results predicted by the classical theories. Table 1 provides a comparison between the classical results and a typical experimental results.

B. The Modern Theories:

The failure of the classical theories to correctly represent the observed thermodynamic behavior near the critical point is attributed to their assumption that attractive forces between molecules are long ranged. In real fluids, however, these forces are usually short ranged. As an attempt to predict the critical behavior of more realistic systems, several theoretical model systems were proposed. The Ising model, the classical Heisenberg model and the spherical model are all well-known model systems with short-ranged forces. The Ising model assumes that each atom on a lattice site either spins up or down (the spin is said to have a dimension of one) and the interaction is between neighboring pairs. The Ising model provides a crude model of ferromagnetism and it also serves as a practical model for many systems such as a one-component fluid (through the lattice-gas), a binary fluid and alloy. The Heisenberg model regards the magnetic moments as being related to quantum-mechanical three-component spin operators (three-dimensional spin), and assumes that the energy is proportional to the scalar product of these operators. The Heisenberg model can be used to describe behaviors of a certain ferromagnets and antiferromagnets. Finally, the spherical model which assumes an infinite dimensionality of spin corresponds to no realistic systems in nature. Unlike the Weiss model of ferromagnetism, the Ising and the Heisenberg model unfortunately have not been solved exactly in three dimensions. Only the two-dimensional Ising model is exactly

TABLE 1: A comparison between typical experimental results and the classical results on the behavior of magnetic and liquid-gas systems near the critical point.

	Typical Experimental Results	Classical Results
Shape of coexistence curve	$(\rho_L - \rho_G) \sim \left \frac{T - T_c}{T_c} \right ^\beta ;$ $\beta = 0.3 - 0.4$	$(\rho_L - \rho_G) \sim \left \frac{T - T_c}{T_c} \right ^{1/2}$
Compressibility or susceptibility	$K_T \text{ or } \chi_T \sim \left(\frac{T - T_c}{T_c} \right)^{-\gamma} ;$ $\gamma = 1.1 - 1.4$	$K_T \text{ or } \chi_T \sim \left(\frac{T - T_c}{T_c} \right)^{-1}$
Specific heat	$C_V \text{ or } C_H \sim \left(\frac{T - T_c}{T_c} \right)^{-\alpha} ;$ $\alpha = 0 - 0.2$	discontinuous

soluble, by the famous Onsager solution done in 1944. The model demonstrates that the specific heat possesses a logarithmic divergence at T_c when approached from both the high and low temperature sides. This is the first theoretical result that contradicts the predictions of the classical theories. The other exactly soluble model is the spherical model which remains the only model that can be solved exactly in three dimensions.

When exact solutions to the Ising and the Heisenberg model failed, approximation methods were sought. Gaunt and co-workers^{3,4} use the high-temperature series method to obtain approximate solutions for the two- and three-dimensional Ising model. Another method is the renormalization group and the ϵ -expansion technique which have been employed by Brezin and co-workers to obtain equation of states for an Ising-like ferromagnet⁵ and a classical Heisenberg ferromagnet.⁶ The results of these approximation methods are moderately successful.

Other attempts to predict an equation of state of a system near the critical point have been done phenomenologically. The NBS equation⁷ and the parametric equation of state⁸ (also known as the linear model) are two well-known examples. As far as creating an equation suitable for comparison with data, their results have been perhaps more successful.

C. This Work

Our work, like much other theoretical work in this area, is concerned with obtaining an equation of state that can describe the behavior of systems near the critical points. The work has been built around the concept of a spinodal--a concept that has been questioned by

some theoretical considerations.

As we have seen earlier, the concept of the spinodal and metastability was first introduced by van der Waals in his classical theory. By definition, a true spinodal curve actually represents the limit of metastability of the one-phase state in the two-phase region. Benedek⁹ used this concept to describe critical region data off the critical isochore. According to the spinodal assumption introduced by Benedek, along any off-critical isochore various thermodynamic and transport properties diverge relative to a spinodal temperature with the same power-law dependence as they exhibit along the critical isochore when the critical temperature is approached. This concept has been discussed extensively by Chu, Schoenes and Fisher.¹⁰ In their paper, Chu et al. have shown that the spinodal assumption would lead to an equation of state that is non-analytic in density on the critical isochore for temperatures greater than the critical temperature. They further showed that the equation of state would also not be analytic in temperature on the critical isotherm. Thus, the equation of state derived from the spinodal concept would fail to meet the analyticity requirements imposed on it.¹¹ Regardless of whether the equation will be smooth enough to fit data, its non-analytic behavior has been the strongest theoretical objection.

Whether a true spinodal curve exists in nature is still questionable. No experiment has been done to directly indicate its existence. On the other hand, experimental data taken in the one-phase region (in the vicinity of the critical point) fit Benedek's spinodal assumption very well, thus, implying the existence of a spinodal curve. Chu et al.¹⁰ find that their light-scattering data support the concept of

a spinodal. This is also true of thermal-diffusivity and diffusion-coefficient data taken by Benedek.⁹ Various other experimental data¹²⁻¹⁴ have shown a similar support. However, whether the spinodal curve implied by these experimental data is the true spinodal (i.e. the limit of metastability) is unknown. For this reason, Chu et al.¹⁰ preferred to call it the "pseudospinodal curve" and Benedek's assumption the "pseudospinodal assumption" a terminology which we shall henceforth use.

In view of all the controversies given above, Sorensen and Semon¹⁵ have recently derived an equation of state by applying the pseudospinodal assumption to the isothermal compressibility. The equation of state they derived works very successfully for liquid-gas systems, fits PVT data as well as other phenomenological equation of state mentioned earlier, and it is very easy to use. From their equation, other thermodynamic functions and their universal amplitude ratios can easily be derived. The equation, however, has two difficulties. First, it only works for liquid-gas systems which are described by the three-dimensional Ising model, but not for other systems. Second, as expected, the equation is not analytic in the one-phase region on the critical isochore and critical isotherm.

The successful results of Sorensen and Semon suggest the usefulness of the pseudospinodal concept in critical phenomena. Their success has been the motivation of our work. Here, we present some more evidence supporting the concept of the pseudospinodal. By revising Benedek's pseudospinodal assumption, we find an equation of state which not only works for the three-dimensional Ising model but for the Heisenberg model systems as well. The revised pseudospinodal assumption is obtained by adding an additional term to the original assumption. The form is

inferred from the known behavior of the isothermal compressibility of the spherical model along the off-critical isochores. The equation of state we derived agrees when compared with other theoretical equations of states, and predict universal amplitude ratios in good agreement with data and other theoretical results. Next, by using available experimental evidence for the binary fluids and the liquid-gas systems, we show that the data when fit to Benedek's pseudospinodal assumption provides evidence for the existence of a universal pseudospinodal.

Before we present the detail of our work, basic theories of critical phenomena and the terminologies that we will use in the later chapters will be given first in the next chapter. In chapter three, we present the revised form of the pseudospinodal assumption and show how the equation of state is derived from it. Derivation of other thermodynamic functions and their critical amplitude ratios are also presented. In chapter four, we give the results of our numerical calculations on the critical amplitude ratios; comparison of our equation of state with other equations is also given. In chapter five, we explain how we have used the available experimental evidence to test the existence of the universal pseudospinodal. Finally, in the last chapter we summarize and discuss the results we obtained.

Chapter 2

BASIC CONCEPTS OF CRITICAL PHENOMENA

The breakdown of the classical theories stimulated new non-classical approaches to critical phenomena. The new approaches were pioneered by Widom,¹⁶ Griffiths,¹¹ and experiments. The non-classical theories culminated in the well-known renormalization group theory. In this chapter, we shall present the new concepts in critical phenomena which have been initially introduced by Widom and later extended by Griffiths.

A. Order Parameter and Order of Phase Transitions:

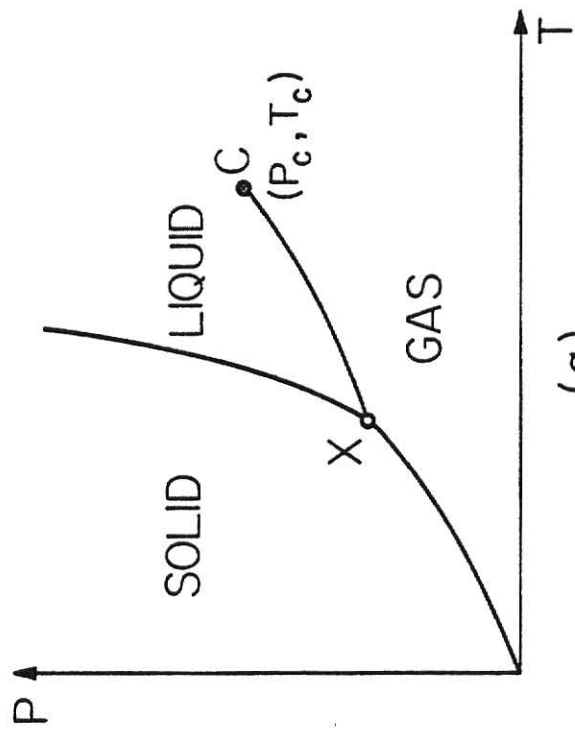
In order to introduce the non-classical concepts we shall consider phase diagrams for typical solid-liquid-gas and ferromagnetic phase transitions.

Figure 3(a) is a pressure versus temperature diagram showing the domains of existence of three phases, solid, liquid and gas. Each point on the three curves in the diagram represents an equilibrium state in which two or more phases can co-exist. The triple point, X, represents an equilibrium state in which all three phases coexist. The critical point, C, is the end point of the vapor pressure curve. By circling round the critical point, one can pass continuously from the liquid to the gaseous phase, without any necessity for a discontinuous transition.

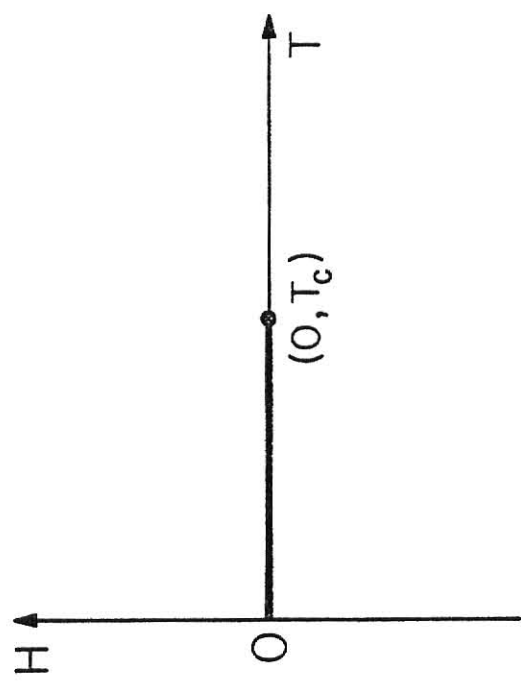
Figure 3(b) is a magnetic field versus temperature diagram for a material undergoing a ferromagnetic phase transition. It exhibits a

FIGURE 3

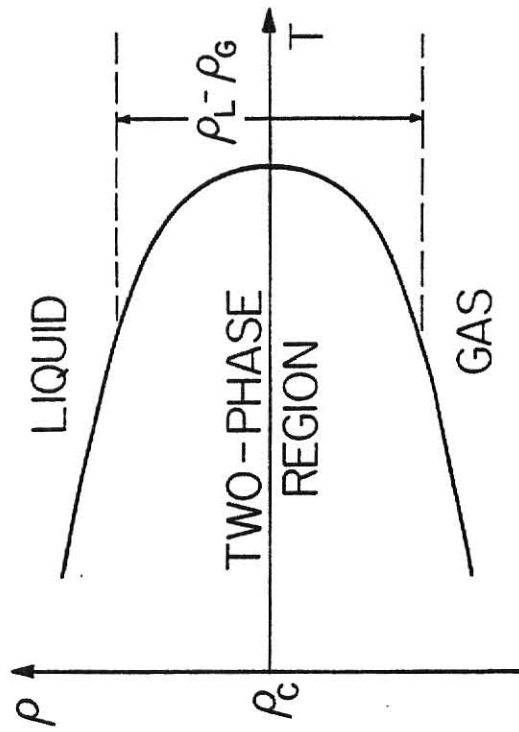
- (a) Typical solid-liquid-gas phase diagram.
- (b) Typical ferromagnetic phase diagram.
- (c) Typical variation of the order parameter $(\rho_L - \rho_G)$ with respect to temperature for the liquid-gas phase transition.
- (d) Typical variation of the order parameter M with respect to temperature for the ferromagnetic phase transition.



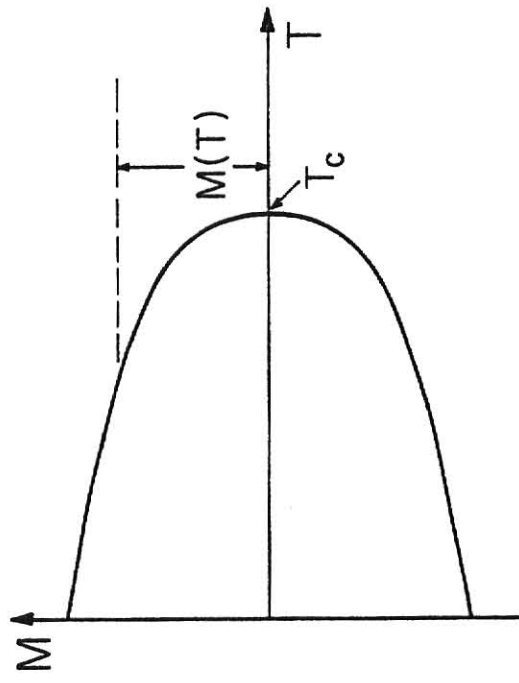
(a)



(b)



(c)



(d)

boundary line along the horizontal axis terminating at the critical point. In zero field and at high temperature, one observes the paramagnetic disordered phase, having no magnetization; as the temperature drops, a transition takes place at the critical point $T = T_c$. For $T < T_c$ one observes the ordered ferromagnetic phase, which is spontaneously magnetized. There is an analogy between this ferromagnetic phase transition and the liquid-to-gas transition; the magnetic field and the pressure play analogous roles. The line XC is analogous to the line $H = 0$ ($0 < T < T_c$).

The most fundamental idea which helps elucidate the behavior near a critical point is the concept that this transition is describable by an order parameter. The main characteristic of the order parameter in any type of phase transition is that it vanishes above the critical point and is nonzero in the region below the critical temperature T_c . In the liquid-gas phase transition, the order parameter is the difference between the liquid and gas densities, $(\rho_L - \rho_G)$. Below the critical temperature T_c , that is in the two-phase region, this quantity is nonzero. As the critical point is approached from below, $(\rho_L - \rho_G)$ gradually decreases in value and becomes zero at the critical point and above it. For a ferromagnetic transition, the order parameter is the homogeneous magnetization, M . In this transition, the magnetization is nonzero in the ordered phase, the ferromagnetic phase, and is zero in value in the disordered phase namely the paramagnetic phase.

When the order parameter has a discontinuity at the transition, one says, following Landau,¹⁶ that one is dealing with a first-order transition; when there is no such discontinuity, the transition is at least second order. In Figure 3(a) and 3(b), the transition lines are

lines of first-order transitions; at the critical points the transition are of second-order. If one plots the measured value of the order parameter as a function of temperature for a second-order transition, one obtains typically curves like the ones shown in Figure 3(c) and 3(d) for the liquid-gas and the ferromagnetic phase transition respectively. Note that in each case there is no discontinuity at T_c in the order parameter, but there is a discontinuity in its slope.

B. Choice of Variables:

For the sake of simplicity, from now on we shall restrict our discussion to the more familiar liquid-gas phase transition. Analogies between fluid and magnet systems will be given whenever it is necessary.

To describe thermodynamic behavior of a fluid system near the critical point, there are two sets of independent variables we may use. One set of the independent variables is volume V and temperature T ; and another set is density ρ (i.e. the number density $\rho = N/V$) and temperature T . If volume and temperature are chosen, then the characteristic thermodynamic potential is the Helmholtz free energy per mole; in this description pressure P and volume V are conjugate variables and the equation of state $P(V, T)$ is obtained by differentiation of the Helmholtz free energy with respect to volume. If density and temperature are used, then the characteristic thermodynamic potential is the Helmholtz free energy per volume; in that description chemical potential μ and density ρ are conjugate variables and the corresponding equation of state $\mu(\rho, T)$ is obtained by differentiation of the Helmholtz free energy with respect to ρ .

Thermodynamics, however, does not uniquely specify which set of variables is to be preferred in describing the critical behavior of fluids.

To make the choice, we consider symmetry properties in the thermodynamic variables. Figure 4 shows the coexistence curve of argon in terms of volume and temperature and in terms of density and temperature. As illustrated in the figure, the coexistence curve, when plotted as a function of density shows considerably more symmetry than when plotted as a function of volume. An equally striking difference in symmetry features is noted above the critical temperature when a $\mu(\rho)$ isotherm is compared with a $P(V)$ isotherm, as illustrated in Figure 5; the $\mu(\rho)$ isotherms are antisymmetric with respect to the point $\rho_c, \mu(\rho_c)$, in contrast to the $P(V)$ isotherms. In the magnetic systems, the spontaneous magnetization is symmetric with respect to the line $M=0$, whereas the magnetic field H is antisymmetric in M .

In view of these symmetry features we shall adopt density ρ and temperature T as the independent variables to describe the behavior of fluids near the critical point. The extensive thermodynamic functions, such as Helmholtz free energy, A , entropy, S , and heat capacity at constant volume, C_V , are therefore taken per unit volume. The equation of state to be considered will be the chemical potential μ , as a function of ρ and T . For ferromagnets, the obvious independent variables are magnetization M and temperature T , and the corresponding equation of state is the magnetic field $H(M, T)$.

In critical phenomena, all thermodynamic properties are made dimensionless by expressing them in units of appropriate combinations of critical parameters. We thus define

$$\begin{aligned}\rho^* &= \rho/\rho_c, \quad T^* = T/T_c, \quad A^* = A/P_c \\ \mu^* &= \mu\rho_c/P_c, \quad P^* = P/P_c, \quad S^* = ST_c/P_c \\ C_V^* &= C_V T_c/P_c, \quad K_T^* = K_T P_c, \quad \chi_T^* = \rho^{*2} K_T^*.\end{aligned}\tag{5}$$

FIGURE 4

The coexistence curve of argon in terms of volume and temperature and in terms of density and temperature. From Ref. 2.

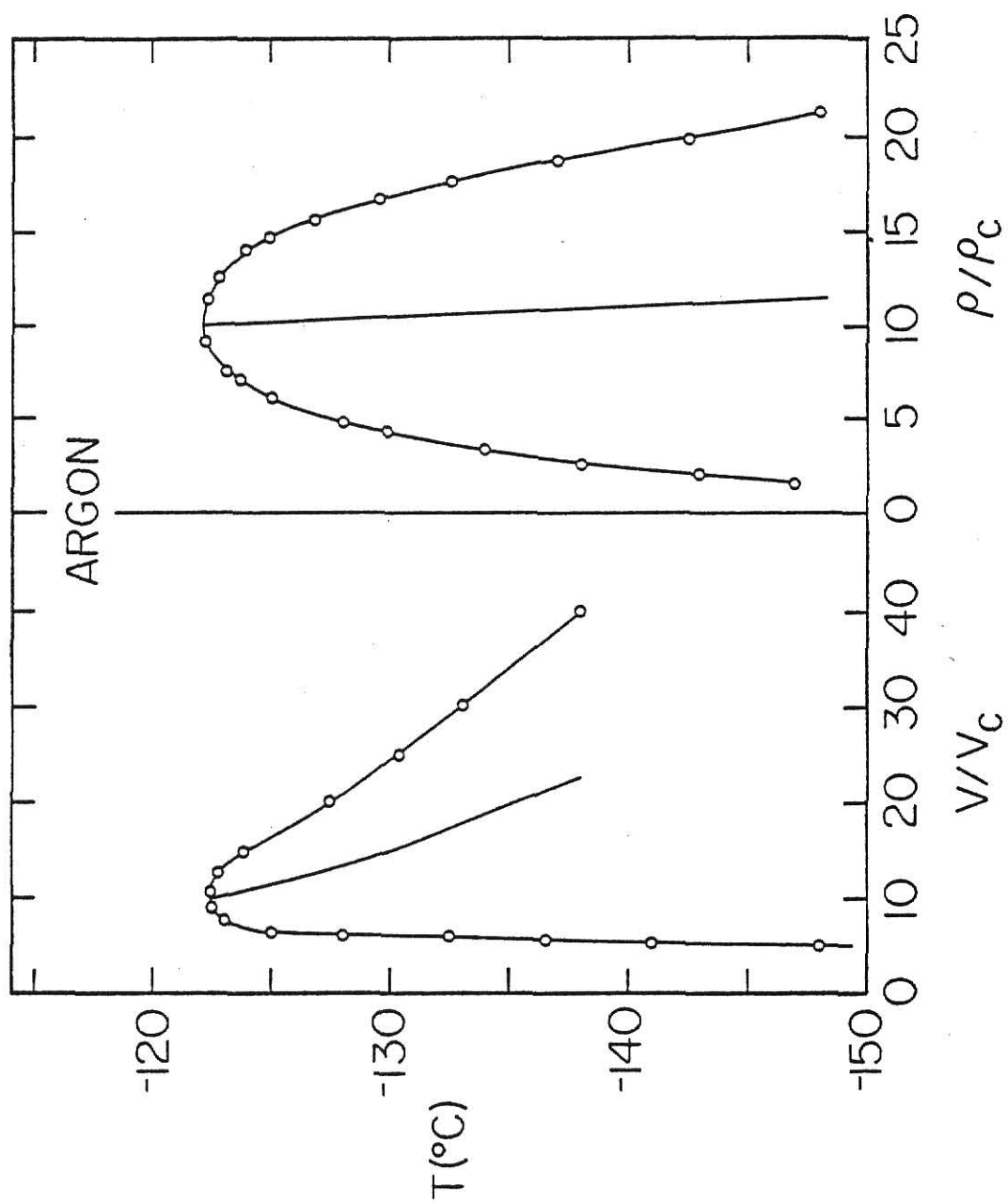
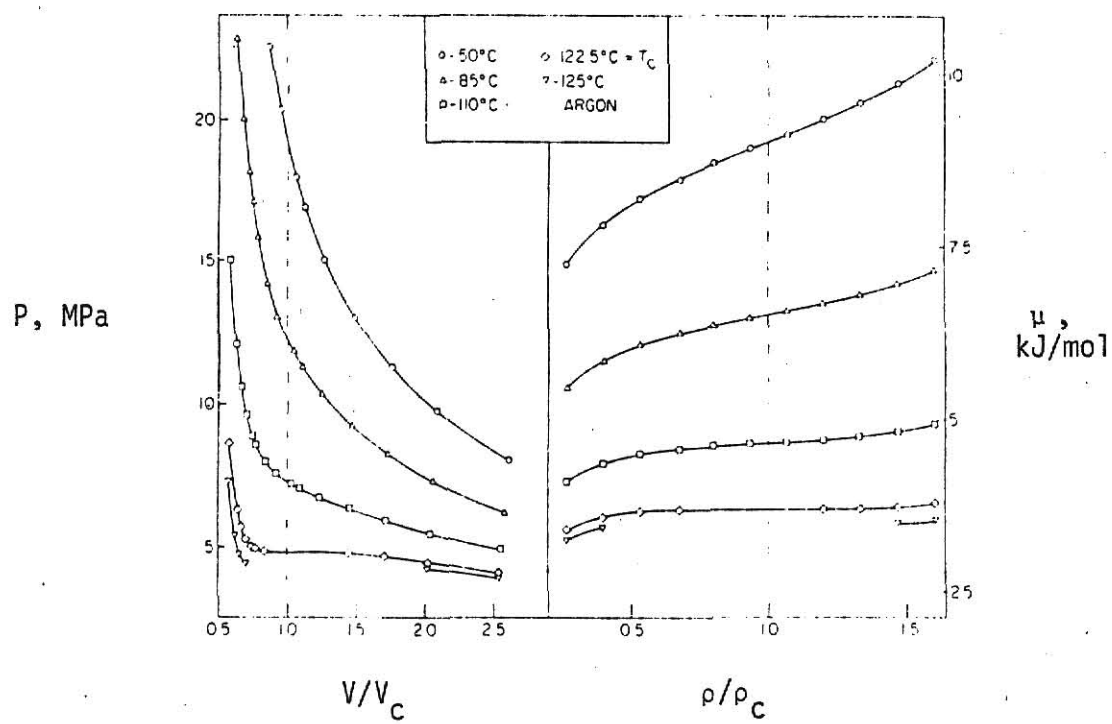


FIGURE 5

$P(V)$ isotherms and $\mu(\rho)$ isotherms of argon in the critical region. In contrast to the $P(V)$ isotherms, the $\mu(\rho)$ isotherms are nearly antisymmetric with respect to ρ_c . From Ref. 2.



The scaled critical density, pressure and temperature are therefore unity by definition. In the above equation, $K_T = -V^{-1} (\frac{\partial V}{\partial P})_T$ is the isothermal compressibility and

$$\chi_T = (\frac{\partial \rho}{\partial \mu})_T = \rho^2 K_T \quad (6)$$

is defined as "the generalized compressibility" or equivalently "the generalized susceptibility" in magnetic language. In addition, we introduce quantities defined with respect to their values at the critical point,

$$\Delta T^* = (T - T_c)/T_c \quad (7a)$$

$$\Delta \rho^* = (\rho - \rho_c)/\rho_c \quad (7b)$$

and the chemical potential difference which is defined as

$$\Delta \mu^* = [\mu(\rho, T) - \mu(\rho_c, T)] \rho_c / P_c \quad (8)$$

where $\mu(\rho_c, T)$ is the chemical potential on the critical isochore at temperature T .

C. Critical-Point Exponents and Power Laws:

In the description of the anomalous critical behavior of a physical property, it is assumed that sufficiently close to the critical point the property varies, to a first approximation, as a simple power of the temperature difference or the density difference from the critical point. The exponent of the power will depend on the property chosen, the path along which the critical point is approached and the way the distance from the critical point is measured. The most commonly used power laws, and also the power laws needed for the purpose of this thesis, for thermodynamic properties are defined as follows:

$$\text{coexistence curve: } \Delta \rho^* = \pm B |\Delta T^*|^\beta \quad (9)$$

$$\text{critical isotherm: } \Delta \mu^* = D (\Delta \rho^*) |\Delta \rho^*|^{\delta-1}, \quad (\Delta T^* = 0) \quad (10)$$

$$\text{compressibility: } \rho^{*2} K_T^* = \Gamma (\Delta T^*)^{-\gamma}, \quad (\rho^* = 1, \Delta T^* > 0) \quad (11a)$$

$$\rho^{*2} K_T^* = \Gamma' |\Delta T^*|^{-\gamma'}, \quad (\text{coexistence curve,} \\ \Delta T^* < 0) \quad (11b)$$

$$\text{specific heat: } C_V^*/T^* = \frac{A}{\alpha} (\Delta T^*)^{-\alpha}, \quad (\rho^* = 1, \Delta T^* > 0) \quad (12a)$$

$$C_V^*/T^* = \frac{A'}{\alpha'} |\Delta T^*|^{-\alpha'}, \quad (\text{coexistence curve,} \\ \Delta T^* < 0) \quad (12b)$$

$$C_V^*/T^* = \frac{A_I}{\alpha''} |\Delta T^*|^{-\alpha''}, \quad (\rho^* = 1, \Delta T^* < 0, \\ \text{two-phase region}) . \quad (12c)$$

In addition to all these, we also introduce the critical-point exponents ν' , ν and η which refer to the behavior of the pair correlation function $G(r)$ of a system in the critical region. Since a rather detailed discussion of this function is given in Reference 1, we give only a brief definition of the exponents themselves here. The correlation length ξ is a measure of the spatial range of the density correlation function. It is assumed that very close to the critical point,

$$\xi = \xi_0 (\Delta T^*)^{-\nu}, \quad (\Delta T^* > 0, \rho^* = 1) \\ = \xi_0' |\Delta T^*|^{-\nu'}, \quad (\Delta T^* < 0, \text{coexistence curve}) . \quad (13)$$

The pair correlation function at $T = T_c$ falls off to zero with distance r with the simple power law form

$$G(r) = e^{-r/\xi} |r|^{-(d-2+\eta)}, \quad (T^* = 1, P^* = 1) . \quad (14)$$

Here d is the dimensionality of the system.

The paths along which all the above power laws are defined, namely the critical isochore $\Delta \rho^* = 0$, the critical isotherm $\Delta T^* = 0$ and the co-

existence curve are schematically indicated in Figure 6.

At one time, many thought that the values of the critical-point exponents were all reciprocal of integers. However, these exponents have now been measured with experimental accuracies that leave no room to doubt that their values are indeed not inverse integers. Values of the exponents α , β , γ , δ , ν and η are given in Table 2 for selected fluid and magnetic systems, and for a few theoretical models. If we study the table, we notice a distinct similarity among the values found experimentally for each exponent despite the fact that the materials are of varied difference in nature. Table 2 also clearly shows the failure of the classical theories to predict the observed values of the exponents. Also failing in this regard are the various exactly soluble models such as the two-dimensional Ising model and the three-dimensional spherical model. On the other hand, the predictions of the three-dimensional Ising model and the three-dimensional Heisenberg model do appear to mirror to a certain extent the data on, respectively, fluid and magnet systems.

The scaling laws to be introduced later impose a number of conditions upon the critical exponents in the power laws. First, as regards the exponents α , γ , ν , their primed values (low-temperature values, $T < T_c$) and unprimed values (high-temperature values, $T > T_c$) are equal.

$$\alpha'' = \alpha' = \alpha, \gamma' = \gamma, \nu' = \nu. \quad (15)$$

Furthermore, between the seven exponents defined above there hold four relations among them. The first three involved only the exponents themselves.

$$2 - \alpha = \beta (\delta + 1) \quad (16a)$$

$$\gamma = \beta (\delta - 1) \quad (16b)$$

$$\gamma = (2 - \eta)\nu \quad (16c)$$

FIGURE 6

Critical exponents for power-law anomalies of thermodynamic properties. The diagram is taken from Ref. 18.

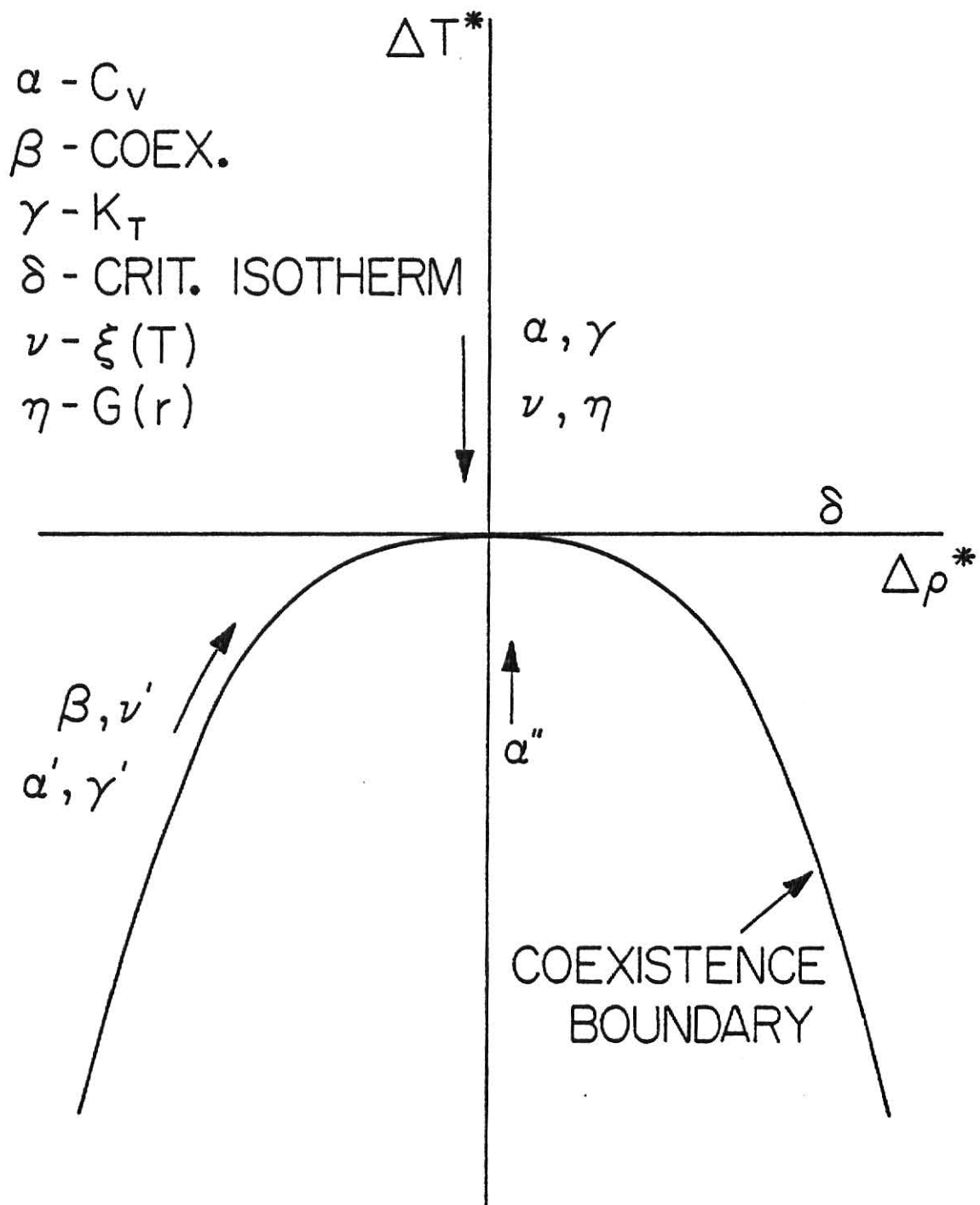


TABLE 2. Values of critical-point exponents for selected systems.

SYSTEMS	CRITICAL EXPONENTS					
	β	δ	α	γ	ν	η
<u>FLUIDS</u>						
CO ₂ ^a	0.321	4.85	0.10	1.24	--	~0
Xe ^a	0.329	4.74	0.11	1.23	--	0.05
SF ₆ ^a	0.321	4.99	0.08	1.28	--	~0
<u>MAGNETS</u>						
Ni ^b	0.375	4.22	0.06	1.31	--	--
EuS ^f	0.360	--	0.05 ^c	1.39 ^f	0.702 ^f	--
CrBr ₃ ^d	0.368	4.31	--	1.215	--	--
<u>SOLUBLE MODELS</u>						
classical	$\frac{1}{2}$	3	discontinuous	1	$\frac{1}{2}$ ^c	0 ^c
d=3 spherical model ^c	$\frac{1}{2}$	5	-1	2	1	0
d=2 Ising model ^c	0.125	15	0 (log)	1.75	1	$\frac{1}{4}$

TABLE 2. Values of critical-point exponents for selected systems. (Continued)

SYSTEMS	CRITICAL EXPONENTS					
	β	δ	α	γ	ν	η
<u>APPROXIMATIONS</u>						
d=3 Ising model ^e	0.3241±0.006	4.82±0.06	0.110±0.008	1.241±0.004	0.63±0.002	0.031±0.011
d=3 Heisenberg model ^e	0.362±0.012	4.82±0.12	-0.115±0.015	1.39±0.01	0.705±0.005	0.031±0.022

- (a) Reference 24
 (b) Reference 25
 (c) Reference 1
 (d) Reference 26
 (e) Reference 27
 (f) Reference 28

while the fourth involves also the dimensionality of space:

$$\nu d = 2 - \alpha \quad . \quad (16d)$$

By virtue of these four relations, the problem of determining the seven critical exponents reduces to determining any two of them.

D. Generalized Homogeneous Functions and the Homogeneity Postulate:

The concept of homogeneity plays a very important role in critical phenomena. As we shall see, the homogeneous function approach leads to scaling laws for thermodynamic functions and thus equation of state of a system, it predicts the power laws introduced in the previous section and also gives the equality relations among the critical exponents, Eq. (15) and Eq. (16). To introduce this concept we consider here functions of two variables only; generalization to functions of more variables is obvious.

A function $f(x,y)$ of two variables x and y is called a homogeneous function if it satisfies the relation

$$f(\lambda^a x, \lambda^b y) = \lambda f(x,y) \quad (17)$$

for two fixed exponents a and b and for all values of the parameter λ .¹

When a function has the property of homogeneity one can always deduce a scaling law, that is the dependence on the two variables can be reduced to the dependence on one new variable by an appropriate change of scale. For this purpose we take $\lambda^a = x^{-1}$ so that

$$\frac{f(x,y)}{x^{1/a}} = f(1, \frac{y}{x^{b/a}}) = f(z) \quad (18a)$$

where for simplicity, we consider only positive values of the variables x and y . Hence, the function $f(x,y)$ after scaling with the factor $x^{1/a}$

becomes a function of the single variable $z = yx^{-b/a}$. Another possible choice is $\lambda^b = y^{-1}$ so that

$$\frac{f(x,y)}{y^{1/b}} = f\left(\frac{x}{y^{a/b}}, 1\right) = f(u) \quad (18b)$$

where $u = xy^{-a/b}$. From Eq. (18) we note that a generalized homogeneous function satisfies a simple power law along any line $xy^{-a/b} = B$

$$f(x,y) = f(B,1) y^{1/b} \quad (19)$$

where $f(B,1)$ is a constant coefficient. In particular, along the special lines $x = 0$ and $y = 0$ the function behaves as

$$f(0,y) = f(0,1) y^{1/b}, \quad f(x,0) = f(1,0) x^{1/a}. \quad (20)$$

The modern description of the thermodynamic behavior of a system near a critical point is based on the assumption of homogeneity of the basic thermodynamic functions. It has been observed experimentally that the singular parts of various thermodynamic properties follow a power law when the critical point is approached along the critical isochore $\Delta p^* = 0$, the critical isotherm $\Delta T^* = 0$ and along the coexistence curve $\Delta p^*/|\Delta T^*|^\beta = \pm B$.

In analogy to Eq. (19) and Eq. (20), the homogeneity postulate assumes that the singular parts of various thermodynamic functions are generalized homogeneous functions of Δp^* and ΔT^* . This postulate was first formulated by Widom¹⁶ for the singular part of the chemical potential. Here, we adopt the formulation of Griffiths¹¹ assuming that the singular part A^* of the Helmholtz free energy in the one-phase region is a generalized homogeneous function of its characteristic variables Δp^* and ΔT^* , that is,

$$A^*(\lambda^a \Delta\rho^*, \lambda^b \Delta T^*) = \lambda A^*(\Delta\rho^*, \Delta T^*) \quad (21)$$

From now on, we assume that any non-singular or the so-called background terms in the $A^*(\Delta\rho^*, \Delta T^*)$ function and other thermodynamic functions have been subtracted off.

The homogeneity property Eq. (21) for A^* implies that the chemical potential difference $\Delta\mu^* = (\partial A^*/\partial\rho^*)_T$, the isothermal compressibility $\chi_T^{*-1} = (\partial\mu^*/\partial\rho^*)_T$, the singular contribution to the entropy $S^* = -(\partial A^*/\partial T^*)_{\rho}$, and the specific heat $C_V^*/T^* = -(\partial^2 A^*/\partial T^{*2})$ are also generalized homogeneous functions of $\Delta\rho^*$ and ΔT^* . After differentiating and redefining the parameter λ appropriately one obtains,¹⁶

$$\Delta\mu^*(\lambda^{a/(1-a)} \Delta\rho^*, \lambda^{b/(1-a)} \Delta T^*) = \lambda \Delta\mu^*(\Delta\rho^*, \Delta T^*) \quad (22a)$$

$$\chi_T^{*-1} (\lambda^{a/(1-2a)} \Delta\rho^*, \lambda^{b/(1-2a)} \Delta T^*) = \lambda \chi_T^{*-1} (\Delta\rho^*, \Delta T^*) \quad (22b)$$

$$S^*(\lambda^{a/(1-b)} \Delta\rho^*, \lambda^{b/(1-b)} \Delta T^*) = \lambda S^*(\Delta\rho^*, \Delta T^*) \quad (22c)$$

$$\frac{C_V^*}{T^*} (\lambda^{a/(1-2b)} \Delta\rho^*, \lambda^{b/(1-b)} \Delta T^*) = \lambda \frac{C_V^*}{T^*} (\Delta\rho^*, \Delta T^*). \quad (22d)$$

Along the critical isochore $\Delta\rho^* = 0$ and along the critical isotherm $\Delta T^* = 0$ these thermodynamic properties will vary according to power laws analogous to Eq. (20). In particular,

$$\chi_T^{*-1} (0, \Delta T^*) = \chi_T^{*-1} (0,1) (\Delta T^*)^{(1-2a)/b} \quad (23a)$$

$$\frac{C_V^*}{T^*} (0, \Delta T^*) = \frac{C_V^*}{T^*} (0,1) (\Delta T^*)^{(1-2b)/b} \quad (23b)$$

$$\Delta\mu^*(\Delta\rho^*, 0) = \pm \Delta\mu^*(1,0) |\Delta\rho^*|^{(1-a)/a} \quad (23c)$$

For the two coexisting phases below the critical temperature $\Delta\mu^* = 0$, while $\Delta\rho^*_{\text{coex.}} \neq 0$. From the homogeneity assumption Eq. (22a) it follows that at the coexistence curve,

$$\Delta\mu^* (|\Delta T^*|^{-a/b} \Delta\rho^*, -1) = 0$$

so that

$$|\Delta T^*|^{-a/b} \Delta\rho^*_{\text{coex.}} = \pm B$$

where B is a constant. The power law behavior of the compressibility and the specific heat along the coexistence curve $\Delta\rho^*/|\Delta T^*|^{a/b} = \pm B$ follows from Eq. (22b) and Eq. (22d) in analogy with Eq. (19)

$$x_T^{*-1} (\Delta\rho^*_{\text{coex.}}, \Delta T^*) = x_T^{*-1} (B, -1) |\Delta T^*|^{(1-2a)/b} \quad (24a)$$

$$\frac{C_V^*}{T^*} (\Delta\rho^*_{\text{coex.}}, \Delta T^*) = \frac{C_V^*}{T^*} (B, -1) |\Delta T^*|^{(1-2b)/b} \quad (24b)$$

We thus have recovered the thermodynamic power laws introduced in the last section with

$$\begin{aligned} \alpha &= \alpha' = (2b - 1)/b, \quad \beta = a/b \\ \gamma &= \gamma' = (1 - 2a)/b, \quad \delta = (1 - a)/a \end{aligned} \quad (25)$$

so that

$$a = \frac{1}{\delta+1} = \frac{\beta}{2-\alpha}, \quad b = \frac{1}{\beta(\delta+1)} = \frac{1}{2-\alpha} \quad (26)$$

Thus, from the last two equations we obtain

$$2 - \alpha = \beta(\delta + 1), \quad \gamma = \beta(\delta + 1)$$

which are the equality relations given in Eq. (16a) and Eq. (16b).

The other two exponent relations given in Eq. (16c) and Eq. (16d) can be obtained by finding the scaling law for the correlation function. This is fully discussed in Reference 1.

E. Scaling Laws for Equation of State and Thermodynamic Functions:

The homogeneity postulate asserts that all thermodynamic functions and thus the equation of state can be expressed in terms of only one variable by proper scaling procedures. Here, we shall apply this postulate to obtain scaling laws for equation of state of a system and its thermodynamic functions.

Consider first the Helmholtz free energy of a system. According to the homogeneity postulate Eq. (21), the Helmholtz free energy satisfies scaling law of the form

$$\frac{A^*(\Delta\rho^*, \Delta T^*)}{|\Delta\rho^*|^{\delta+1}} = A^*(1, x) \quad (27)$$

The above expression is obtained by letting $\lambda^a = (\Delta\rho^*)^{-1}$ and using $a = 1/(\delta + 1)$, Eq. (26). Notice that A^* is indeed a function of one variable, x , when scaled by the quantity $|\Delta\rho^*|^{\delta+1}$. The variable x is called the scaling variable and is defined as

$$x = \Delta T^* / |\Delta\rho^*|^{1/\beta} \quad (28)$$

By introducing a new function $a(x)$ we can rewrite A^* as

$$A^*(\Delta\rho^*, \Delta T^*) = |\Delta\rho^*|^{\delta+1} a(x) \quad (29)$$

The chemical potential difference $\Delta\mu^*(\Delta\rho^*, \Delta T^*)$, can be obtained by redefining the parameter λ in Eq. (22a). By letting $\lambda^{a/(1-a)} = (\Delta\rho^*)^{-1}$ and using the values of a and b in Eq. (26), we obtain

$$\frac{\Delta\mu^*(\Delta\rho^*, \Delta T^*)}{|\Delta\rho^*|^\delta} = \Delta\mu^*(1, x) \quad . \quad (30)$$

A new function $h(x)$ is introduced in place of $\Delta\mu^*(1, x)$; thus we obtain a scaled equation of state of the form

$$\Delta\mu^*(\Delta\rho^*, \Delta T^*) = |\Delta\rho^*|^\delta h(x) \quad . \quad (31)$$

Since $\Delta\mu^* = (\partial A^*/\partial \Delta\rho^*)_T$, the scaling function $h(x)$ is related to the scaling function $a(x)$ for the free energy by

$$\beta h(x) = -x a'(x) + \beta(\delta + 1) a(x) \quad (32)$$

where the prime denotes differentiation with respect to x .

The scaled equation for the compressibility $\chi_T^{*-1} = (\partial\mu^*/\partial\rho^*)_T$ follows immediately from Eq. (31)

$$\chi_T^{*-1} = |\Delta\rho^*|^{\delta-1} \left[\delta h(x) - \frac{x}{\beta} \frac{dh(x)}{dx} \right] \quad . \quad (33)$$

Thus we see that the compressibility is a function of the variable x only, when scaled by the quantity $|\Delta\rho^*|^{\delta-1}$.

The scaling function $h(x)$ and the scaled variable x merit further discussion. $x = \Delta T^*/|\Delta\rho^*|^{1/\beta}$ assumes the value $-x_0$ at the phase boundary, the value 0 on the critical isotherm and the value $+\infty$ on the critical isochore. Since the chemical potential is a constant along any isotherm in the two-phase region, $\Delta\mu^* = 0$ at the coexistence and, thus, $h(-x_0) = 0$. The function $h(x)$ becomes infinite at the critical isochore. In addition to the boundary conditions $h(-x_0) = 0$ and $h(\infty) = \infty$, the function $h(x)$ is restricted by several conditions, formulated by Griffiths.¹¹ These conditions arise first of all from the requirements of thermodynamic stability. Thus, for the compressibility

to be positive, it is necessary that

$$\beta \delta h(x) \geq x \frac{dh(x)}{dx} , \quad (34)$$

as follows from Eq. (33). Additional conditions are imposed on $h(x)$ by the assumption that $\mu(\rho, T)$ is an analytic function throughout the one-phase region with the exception of the critical point and perhaps the phase boundary. The relation Eq. (31) then implies that $h(x)$ has to be analytic in x in the range $-x_0 < x < \infty$; it can, therefore, be expanded in power series in x at every point in this range.

From Eq. (29) and Eq. (31), scaled equations for other thermodynamic functions can be obtained. For the purpose of this thesis, we present the expressions for the scaled entropy and heat capacity in the one-phase region which are of the forms

$$-S^* = |\Delta\rho^*|^{(1-\alpha)/\beta} a'(x) , \quad (35)$$

and

$$-C_V^*/T^* = |\Delta\rho^*|^{-\alpha/\beta} a''(x) , \quad (36)$$

respectively.

F. Universality:

The theoretical studies of various model systems have led to the formulation of the hypothesis of universality. This hypothesis greatly reduces the variety of different types of critical behavior by dividing all systems into a small number of equivalent classes called universality classes. The hypothesis of universality states that systems belonging to the same universality class are expected to have identical

critical exponents and scaling functions and thus obey the same scaled equation of state.¹⁹⁻²¹ It further states that these critical exponents and scaling functions depend^{19,22} on: (a) the lattice or space dimensionality d of a system, (b) the symmetry of the order parameter, and (c) the spin dimensionality n of the system. This means, for example, the exponents and scaling functions for the three-dimensional Ising model denoted by $(d = 3, n = 1)$ are different from those for the $(d=3, n=3)$ Heisenberg model.

The fact that systems in the same universality class have identical critical exponents are convincingly demonstrated by Table 2. The Guggenheim plot displayed in Figure 2 experimentally supports this hypothesis. It shows that the eight different fluids (Ne, Ar, Kr, Xe, N_2 , O_2 , CO, CH_4) belong to the same universality class. The hypothesis is also strongly supported by the renormalization group theory of critical phenomena.²³

The principle of universality also implies universality of the amplitude ratios Γ/Γ' , ξ_0/ξ_0' and A/A' ,²³ (see Eqs. (11), (12), and (13)). Thus the (3,1) Ising model should have amplitude ratios different from the (2,1) Ising model and the (3,3) Heisenberg model. A more detailed study of this subject will be presented in a later chapter.

Chapter 3

DERIVATION OF THE EQUATION OF STATE FROM THE PSEUDOSPINODAL ASSUMPTION

The concept of the pseudospinodal has been briefly introduced in Chapter 1. Here, a further discussion of the concept is given. We shall first restate the pseudospinodal assumption initially introduced by Benedek.⁹ According to Benedek, a given transport or thermodynamic property, X , of a system along any isochore ρ diverges as

$$X = X_0 \{(T - T_S(\rho))/T_C\}^{-x} \quad (37)$$

as the pseudospinodal temperature $T_S(\rho)$ is approached. X_0 and x in Eq. (37) are the same critical amplitude and exponent found along the critical isochore. Note that along the critical isochore ρ_c , $T_S(\rho_c) = T_C$. Under this assumption, the shape of the pseudospinodal curve is found to have the following form

$$\Delta\rho_S^* = B_S \{(T_C - T_S(\rho))/T_C\}^{\beta^+} \quad (38)$$

where B_S is the amplitude of the curve. As pointed out by Chu et al.,¹⁰ it is expected from the concept of homogeneity and scaling that $\beta^+ = \beta$, the exponent describing the coexistence curve.

Despite the strong theoretical objection of nonanalyticity mentioned in Chapter 1, the pseudospinodal assumption has proven to be useful in describing critical phenomena. Benedek,⁹ Chu et al.¹⁰ and other

workers¹²⁻¹⁴ found that the assumption given by Eq. (37) described very well their fluid data along the off-critical isochores. Subsequently, Sorensen and Semon¹⁵ showed that this assumption could be used to derive an equation of state and universal amplitude ratios of systems near the critical points. Their equation compare favorably to fluid data (He^4 and Xe); the universal amplitude ratios they obtained for the fluid systems are in good agreements with experimental values and other theoretical results.

The equation of Sorensen and Semon, however, does not work for systems of other universality classes. The universal amplitude ratios they predicted for the universality classes (2,1), (3,2), and (3,3) do not compare well with data.³⁷ Apparently, Benedek's pseudospinodal assumption works only for the universality class (3,1). Hence, to obtain a pseudospinodal assumption that works for all universality classes, we obviously need to revise the original pseudospinodal assumption. Since the spherical model ($3, n \rightarrow \infty$) is exactly soluble and the behavior of its isothermal compressibility or susceptibility is well-known, it is most reasonable that we deduce a revised pseudospinodal assumption from it.

In this chapter, we present the revised pseudospinodal assumption and give a detailed derivation of the equation of state.

A. The Spherical Model:

Consider the scaled equation of state (see Eq. (31)) for the spherical model,

$$\Delta\mu^*(\Delta\rho^*, \Delta T^*) = |\Delta\rho^*|^\delta h_{sm}(x)$$

derived by Joyce.³⁰ According to his derivation, the scaling function $h_{sm}(x)$ for the spherical model is given by

$$h_{sm}(x) = \left(\frac{x}{x_0} + 1\right)^\gamma \quad (39)$$

where $-x_0$ is the value of x on the coexistence curve. For this model, the spinodal curve and the coexistence curve coincide,³⁰ therefore, $x_0 = x_1$ where x_1 , by definition,³¹

$$x_1 = |\Delta\rho^*|^{-1/\beta} \{(T_c - T_s(\rho))/T_c\} \quad (40)$$

is the value of x on the pseudospinodal curve. Hence, without affecting Eq. (39), we can write $h_{sm}(x)$ as

$$h_{sm}(x) = (x/x_1 + 1)^\gamma \quad (41)$$

As seen from the preceeding chapter, the scaled expression for the isothermal compressibility is related to the scaling function $h(x)$ according to Eq. (33). Using Eq. (33) and (41) we find

$$x_T^{*-1} = \frac{|\Delta\rho^*|^{\delta-1}}{x_1^\gamma} \{(x + x_1)^\gamma + x_1(\delta - 1)(x + x_1)^{\gamma-1}\} \quad (42)$$

If we now replace x_1 and x in the above equation by their respective values and also note that

$$x = |\Delta\rho^*|^{-1/\beta} (T - T_c)/T_c = |\Delta\rho^*|^{-1/\beta} \{(T - T_s(\rho))/T_c + (T_s(\rho) - T_c)/T_c\} \quad (43)$$

we obtain

$$x_T^{*-1} = x_1^{-\gamma} [\{(T - T_s(\rho))/T_c\}^\gamma + x_1(\delta - 1)\Delta\rho^{*1/\beta} \{(T - T_s(\rho))/T_c\}^{\gamma-1}] \quad (44)$$

Along the critical isochore ($\Delta\rho^* = 0$), Eq. (44) becomes

$$x_1^{*-1} = x_1^{-\gamma} \{(T - T_c)/T_c\}^\gamma. \quad (45)$$

Comparison of this equation with Eq. (11a) gives $x_1^\gamma = r$, the amplitude of the isothermal compressibility. Thus, for the spherical model, the isothermal compressibility along the off-critical isochores behaves like

$$x_1^{*-1} = \frac{1}{r} \{(T - T_s(\rho))/T_c\}^\gamma + (\delta-1)(x_1/r)\Delta\rho^{*1/\beta} \{(T - T_s(\rho))/T_c\}^{\gamma-1}. \quad (46)$$

We may call Eq. (46) the pseudospinodal assumption for the spherical model. Note that if the second term is zero, Eq. (46) reduces to the Benedek assumption,

$$x_1^{*-1} = \frac{1}{r} \{(T - T_s(\rho))/T_c\}^\gamma. \quad (47)$$

The fact that the spherical model has a different pseudospinodal assumption suggests that the form of the pseudospinodal assumption is unique to each model system. Equation (46) also suggests that the original pseudospinodal assumption is best revised by adding an extra or correction term to it. The most reasonable correction term to use is the second expression in Eq. (46), since it is homogeneous and of the same order of homogeneity as the first term (i.e. the original assumption). However, note that the term $(\delta-1)$ in the expression is a universal quantity and thus depends only on each universality class.

We shall replace $(\delta-1)$ with an adjustable parameter C in the event that C is not equal to $(\delta-1)$ for other universality classes. Notice that the original assumption is revived by choosing $C = 0$.

B. Derivation of $h(x)$ from the Revised Pseudospinodal Assumption:

Thus, following the above discussion, the pseudospinodal assumption we shall use in deriving the scaling function $h(x)$ is given by

$$x_T^{*-1} = \frac{1}{T} \{ (T - T_S(\rho)) / T_C \}^\gamma + C(x_1/\Gamma) |\Delta\rho^*|^{1/\beta} \quad (48)$$

$$\{ (T - T_S(\rho)) / T_C \}^{\gamma-1} .$$

The generalized compressibility x_T^* is related to the scaling function $h(x)$ according to Eq. (33). We find it beneficial to rewrite the relation here, which is as follows

$$x_T^{*-1} = |\Delta\rho^*|^{\delta-1} \{ \delta h(x) - \frac{x}{\beta} h'(x) \} .$$

If we now compare this expression with Eq. (48), we obtain a first order differential equation for $h(x)$:

$$h'(x) - (\beta\delta/x)h(x) = \frac{\omega}{x}(1 + x/x_1)^\gamma + (C\omega/x)(1 + x/x_1)^{\gamma-1} \quad (49)$$

with $\omega = -\beta x_1^\gamma / \Gamma$.

Equation (49) has a homogeneous solution $kx^{\beta\delta}$, with k a constant of integration to be determined by the boundary conditions. The general solution to Eq. (49) is

$$h(x) = x^{\beta\delta} \{ k + \omega(-1)^{\beta\delta} x_1^{-\beta\delta} \int^z u^{-\beta\delta-1} (1-u)^\gamma du \quad (50)$$

$$+ \omega C(-1)^{\beta\delta} x_1^{-\beta\delta} \int^z u^{-\beta\delta-1} (1-u)^{\gamma-1} du \}$$

where $z = -x/x_1$.

For typical values of $\beta \sim 0.32$ and $\delta \sim 4.5$, the integrals in this equation diverge if we try to make the lower limit of each integral

zero. However, we can temporarily impose the condition $\text{Re}(\beta\delta) < 0$ so that we can make the lower limit in both integrals to be zero and identify them as the incomplete Beta functions. Next we can equate each integral with the appropriate hypergeometric series in the region $\text{Re}(\beta\delta) < 0$ and then analytically continue each series back into the region $\text{Re}(\beta\delta) > 0$. Thus, the solution to the differential equation (47) becomes

$$\begin{aligned} h(x) = & kx^{\beta\delta} + (x_1^\gamma/\delta\Gamma) {}_2F_1(-\beta\delta, -\delta; 1-\beta\delta; z) \\ & + (Cx_1^\gamma/\delta\Gamma) {}_2F_1(-\beta\delta, 1-\delta; 1-\beta\delta; z) \end{aligned} \quad (51)$$

where ${}_2F_1$ is the hypergeometric function. The fact that Eq. (51) is the solution to the differential equation (49) can be verified by substitution. (See Eq. (22) on p. 102 and Eq. (4) on p. 101 of Erdélyi.³²)

There are several conditions that $h(x)$ has to satisfy, which are (i) it has to be real, (ii) it must be continuous across $z = -1$ ($x = x_1$), and (iii) as $x \rightarrow \infty$ ($z \rightarrow -\infty$), $h(x)$ should approach x^γ . Condition (ii) can be met by using an analytic continuation formula for the hypergeometric series (Eq. (2), p. 108 of Erdélyi). This continuation procedure plus the third condition determines the constant k . Thus, the resulting equation of state is

$$\begin{aligned} h(x) = & (x_1^\gamma/\delta\Gamma) [\{\Gamma(1-\beta\delta)\Gamma(\beta)/\Gamma(-\gamma)\} \{1 - C/(\delta-1)\} z|z|^{\beta\delta-1} \\ & + {}_2F_1(-\beta\delta, -\gamma; 1-\beta\delta; z) + C {}_2F_1(-\beta\delta, 1-\gamma; 1-\beta\delta; z)] \end{aligned} \quad (52a)$$

, $|z| \leq 1$

$$= (x_1^\gamma/\delta\Gamma) [\delta(-z)^\gamma {}_2F_1(-\gamma, \beta; 1+\beta; z^{-1}) -$$

$$C\beta\delta \{ \Gamma(-1-\beta)/\Gamma(-\beta) \} (-z)^{\gamma-1} {}_2F_1(1-\gamma, 1+\beta; 2+\beta; z^{-1})] \quad (52b)$$

$$, |z| \geq 1$$

where Eq. (52b) is the analytic continuation of solution (52a) into the region $|z| > 1$. In the above equation $\Gamma(y)$ is the gamma function which should not be confused with the amplitude of the isothermal compressibility r .

Equation (52) with the choice of $C = 0$ gives the equation of state, derived by Sorensen and Semon,¹⁵ which works for the (3,1) universality class. In their paper, Sorensen and Semon have shown that in the classical limit this equation ($C = 0$) reduces to the mean-field or the van der Waals equation of state,

$$h(x) = \frac{1}{r} (x_0 + x) , \quad (53)$$

when its corresponding exponents $\beta = \frac{1}{2}$, $\gamma = 1$ and $\delta = 3$ are substituted into the equation. Thus, the equation of state derived from the pseudo-spinodal assumption is at least reasonable since it reduces to the proper classical limit. Obviously, the choice of $C = (\delta-1)$ yields the equation of state for the spherical model (Eq. (41)) when the spherical model critical exponents $\beta = \frac{1}{2}$, $\delta = 5$ and $\gamma = 2$ are substituted into Eq. (52). In the next chapter, we shall test Eq. (52) to see if it works for other model systems when the critical exponents of each model system are used and the parameter C is properly adjusted.

C. Universal Amplitude Ratios: $\Gamma/\Gamma', \xi_0/\xi_0'$ and R_χ

This section is concerned with the derivation of $\Gamma/\Gamma', \xi_0/\xi_0'$, and R_χ . A/A' will be treated separately; its detailed derivation will

be presented in the next section.

To obtain Γ/Γ' , we express the inverse isothermal compressibility on the coexistence curve in two ways. First, if the critical point is approached from below along the coexistence curve, then the usual relation is $(K_T^* \rho^{*2})^{-1} \equiv \chi_T^{*-1} = \frac{1}{\Gamma'} |\Delta T^*|^\gamma$. Another independent expression that is also valid on the coexistence curve is the pseudospinodal assumption Eq. (48). If we equate these two we find

$$\Gamma/\Gamma' = (x_1/x_0 - 1)^{\gamma-1} \{(x_1/x_0)(1+C) - 1\}. \quad (54)$$

Relations analogous to Γ/Γ' can be obtained for other parameters diverging on the isothermal compressibility pseudospinodal defined by x_1 . This is easily done by generalizing Eq. (54). For example, the correlation length satisfies the equation

$$\xi_0/\xi_0' = (x_1/x_0 - 1)^{\nu-1} \{(x_1/x_0)(1+C) - 1\}. \quad (55)$$

However, this generalization procedure does not work for A/A' . Sorensen and Semon¹⁵ found that the equation similar to Eq. (54) did not yield values for A/A' consistent with the relation they obtained from another alternative derivation of A/A' , which we shall present in the next section.

We next consider R_χ which is given by²⁴

$$R_\chi = D\Gamma B^{\delta-1}, \quad (56)$$

and is also expected to be a universal quantity. In the above equation, $D = h(0)$, Γ is the compressibility amplitude, and B is the amplitude of the coexistence curve. From Eq. (52), we find

$$D = (x_1^\gamma/\delta\Gamma)(1+C). \quad (57)$$

Substituting the above value of D into Eq. (54) yields

$$R_x = \delta^{-1} (1+C)(x_1/x_0)^{\gamma} . \quad (58)$$

Notice that all the three relations, equations (54), (55) and (58) contain x_1/x_0 . Since $h(-x_0) = 0$ and $z = -x/x_1$, the inverse of x_1/x_0 is the zero of the equation of state Eq. (52) and is uniquely determined by β , δ and C , therefore making it a constant for each universality class and thus a universal quantity. We also note that the three amplitude ratios r/r' , ξ_0/ξ_0' and R_x are all uniquely determined by β , δ and C and the zero of the equation of state. Thus, they are universal for systems within a universality class. As we will see in the next section, this is also true of the ratio A/A' .

D. Derivation of A/A' :

The derivation of A/A' is straight forward but is rather tedious. The ratio A/A' is related to the specific heat C_v at constant volume which is in turn derivable from the Helmholtz free energy.

To derive A/A' , we shall first consider the singular or the scaled part of the free energy given by Eq. (29) which is

$$A^*(\Delta\rho^*, \Delta T^*) = |\Delta\rho^*|^{\delta+1} a(x)$$

and shall first evaluate the scaling function $a(x)$. Since $a(x)$ is related to $h(x)$ by the differential equation (32), it can be derived from the equation of state Eq. (52). We find that this differential equation,

$$\beta h(x) = -x a'(x) + \beta(\delta+1)a(x)$$

has the following simple solution

$$a(x) = K x^{2-\alpha} + x^{2-\alpha} \int_0^\infty y^{\alpha-3} h(y) dy \quad (59)$$

where $\alpha = 2-\beta(\delta+1)$ and K is the constant of integration. The integration in Eq. (59) is easily evaluated since $h(x)$ is given by simple power series specifically the hypergeometric series ${}_2F_1$. However, special care has to be taken in the limit as x approaches zero, since in this limit the integral is divergent. In order to make the integral in Eq. (59) convergent, we need to subtract off the homogeneous term in $h(x)$ plus the first few terms in the hypergeometric series expansion. It is found that the total number of terms to be excluded from the integral depends on the value of the exponent α . For $0 < \alpha < 1$, we find

$$\begin{aligned} a(x) = & Kx|x|^{1-\alpha} + h_0 x|x|^{\beta\delta-1} + \frac{\beta h_1}{(2-\alpha)} \\ & + \frac{\beta h_2 x}{(1-\alpha)} + \beta x|x|^{1-\alpha} \int_x^\infty y^{\alpha-3} \{h(y) - h_0 y^{\beta\delta} \\ & - h_1 - h_2 y\} dy \end{aligned} \quad (60)$$

where from Eq. (52) we obtain

$$h_0 = -(x_1^\gamma / \delta \Gamma) \{ \Gamma(1-\beta\delta) \Gamma(\beta) / \Gamma(-\alpha) \} [1 - C/(\delta-1)] x_1^{-\beta\delta} \quad (61a)$$

$$h_1 = (x_1^\gamma / \delta \Gamma) (1+C) \quad (61b)$$

$$h_2 = -(x_1^\gamma / \delta \Gamma) \{ (-\beta\delta)(-\alpha)/(1-\beta\delta) + C(-\beta\delta)(1-\alpha)/(1-\beta\delta) \} . \quad (61c)$$

Following Griffiths,¹¹ the constant K is determined from the fact that $h(x)$ and $a(x)$ should have the same analyticity properties. Requiring that $a(x)$ has the same behavior as $h(x)$ as x approaches zero, we consequently get

$$K = -\beta \int_0^\infty y^{\alpha-3} \{h(y) - h_0 y^{\beta\delta} - h_1 - h_2 y\} dy . \quad (62)$$

Equations (60) and (62) are completely analogous to those of Griffiths,¹¹ the difference being proper accounting for the homogeneous term h_0 . We can get similar expressions for the value of $\alpha < 0$ by subtracting off the third term in each hypergeometric series expansion of Eq. (52).

Since $C_V^*/T^* = -\partial^2 A^*(\Delta\rho^*, \Delta T^*)/\partial \Delta T^{*2}$, the scaled specific heat in the one-phase region is given by

$$-C_V^*/T^* = |\Delta\rho^*|^{-\alpha/\beta} a''(x)$$

which is Eq. (36) in Chapter 2. Differentiating Eq. (60) twice with respect to x and taking the limit as $x \rightarrow \infty$, we obtain

$$a''(x) = K(2-\alpha)(1-\alpha)x^{-\alpha} . \quad (63)$$

If we now substitute Eq. (63) into Eq. (36) and use the fact that $x = \Delta T^*/\Delta\rho^{*1/\beta}$, the specific heat in the one-phase region becomes

$$\frac{C_V^*}{T^*} = -K(2-\alpha)(1-\alpha)\Delta T^{*- \alpha} \quad (64)$$

where the constant K is given by Eq. (62). In the one-phase region, the singular specific heat also satisfies the power law relation $C_V^*/T^* = \frac{A}{\alpha} (\Delta T^*)^{-\alpha}$ (Eq. (12a)). Equating this relation with the above equation and solving for A gives

$$A = \alpha\beta(2-\alpha)(1-\alpha) \int_0^\infty y^{\alpha-3} \{h(y) - h_0 y^{\beta\delta} - h_1 - h_2 y\} dy \quad (65)$$

for $0 < \alpha < 1$.

In the two-phase region, the specific heat has the following scaling form

$$-\frac{C_V^*}{T^*} = (2-\alpha)(1-\alpha)(-\Delta T^*)^{-\alpha} x_0^{\alpha-2} a(-x_0) . \quad (66)$$

Equation (66) is trivially derived by using

$$A^*(\Delta\rho^*, \Delta T^*) = |\Delta\rho^*|^{\delta+1} a(-x_0) \quad (67)$$

which is the free energy on the coexistence curve, and realizing that on the coexistence curve $\Delta\rho^*$ is a function of ΔT^* , that is

$$\Delta\rho^* = \left(\frac{\Delta T^*}{-x_0}\right)^\beta . \quad (68)$$

The relation then is readily obtained by taking the derivative of Eq. (67) twice with respect to ΔT^* . Similarly, in the two-phase region the specific heat along the coexistence curve obeys the power-law relation $C_V^*/T^* = \frac{A'}{\alpha} |\Delta T^*|^{-\alpha}$ (Eq. (12b)). This relation and Eq. (66) when solved yields the expression for A' which is given by

$$A' = -(2-\alpha)(1-\alpha) \alpha x_0^{\alpha-2} a(-x_0) . \quad (69)$$

For $0 < \alpha < 1$, we find

$$\begin{aligned} A' = & \alpha\beta(2-\alpha)(1-\alpha) x_0^{\alpha-2} \left[\frac{h_0 x_0^{\beta\delta}}{\beta} - \frac{h_1}{(2-\alpha)} + \frac{h_2 x_0}{(1-\alpha)} \right. \\ & \left. + x_0^{2-\alpha} \int_{-x_0}^0 |y|^{\alpha-3} \{h(y) - h_0 y |y|^{\beta\delta-1} - h_1 - h_2 y\} dy \right] . \end{aligned} \quad (70)$$

Hence, to obtain A/A' we merely divide Eq. (65) by Eq. (70).

These expressions, Eq. (65) and (70), are completely analogous to those of Barmatz et al.³³ for $0 < \alpha < 1$, the only difference being our treatment of the homogeneous term h_0 . Numerical calculation of A/A' will be described and the results obtained will be given in the next chapter.

Chapter 4

NUMERICAL CALCULATION AND RESULTS

In this chapter, we test to see if our proposed form for the equation of state, Eq. (52), provides a good representation of the following model systems: the (3,1), (3,2), (3,3), and the (2,1). We first compare our predicted universal amplitude ratios to data and other theoretical results. Then, we compare our equation of state to other theoretical equations which are known to represent the model systems reasonably well. Before these comparisons can be made, our initial task is to find the parameter C for each model system. Indeed, there are several ways in which C can be determined. We have chosen a simple and fairly reliable method of obtaining C which we shall present in the next section.

A. Numerical Calculation:

To numerically calculate $h(x)$ and the universal amplitude ratios, we replace the hypergeometric functions in Eq. (52) by their explicit representations. Equation (52) then becomes

$$\begin{aligned} h(x) = & (x_1^\gamma / \delta \Gamma) [\{\Gamma(1-\beta\delta)\Gamma(\beta) / \Gamma(-\gamma)\} \{1 - C/(\delta-1)\} z |z|^{\beta\delta-1} \\ & - \beta\delta \sum_{n=0}^{\infty} \frac{(-\gamma)_n}{(n-\beta\delta)} \frac{z^n}{n!} - \beta\delta C \sum_{n=0}^{\infty} \frac{(1-\gamma)_n}{(n-\beta\delta)} \frac{z^n}{n!}] , \quad |z| \leq 1 \end{aligned} \quad (71a)$$

$$\begin{aligned}
&= (x_1^\gamma / \delta \Gamma) [\delta(-z)^\gamma \sum_{n=0}^{\infty} \frac{(-\gamma)_n}{(n+\beta)} \frac{z^{-n}}{n!} - \beta \delta C \{\Gamma(-1-\beta)/\Gamma(-\beta)\} \\
&\quad (-z)^{\gamma-1} (1+\beta) \sum_{n=0}^{\infty} \frac{(1-\gamma)_n}{(n+\beta+1)} \frac{z^{-n}}{n!}] , \quad |z| \geq 1
\end{aligned} \tag{71b}$$

where in general

$$(x)_n = \Gamma(n+x)/\Gamma(x) \quad .$$

In the above equation, the term $x_1^\gamma / \delta \Gamma$ depends on the detail of each physical system under study, implying that $h(x)$ is not universal. However, if we divide $h(x)$ by this term, $\hat{h}(x) = h(x)/(x_1^\gamma / \delta \Gamma)$ becomes a universal function, and is called a scaled equation of state. If C for each universality class has been found beforehand, $\hat{h}(x)$ is completely determined by the universal quantities β and δ . As far as the values of β and δ are concerned, we have used the most recent theoretical results^{34,35} which are as follows: $\beta = 0.324 \pm 0.006$ and $\delta = 4.82 \pm 0.06$ for the (3,1) model; $\beta = 0.346 \pm 0.009$ and $\delta = 4.81 \pm 0.08$ for the (3,2) model; and $\beta = 0.362 \pm 0.012$ and $\delta = 4.82 \pm 0.12$ for the (3,3) model system. For the (2,1) model, we have used $\beta = 0.125$ and $\delta = 15$,³⁶ which are also the values used by Gaunt and Domb.³

To calculate the universal amplitude ratios we need to know x_0/x_1 , which is the zero of the equation of state. x_0/x_1 is determined using the condition $h(-x_0) = 0$, i.e.,

$$\begin{aligned}
& -\{\Gamma(1-\beta\delta)\Gamma(\beta)/\Gamma(-\gamma)\}\{1 - C/(\delta-1)\} \left|\frac{x_0}{x_1}\right|^{\beta\delta} + \\
& {}_2F_1(-\beta\delta, -\gamma; 1-\beta\delta; \frac{x_0}{x_1}) + C {}_2F_1(-\beta\delta, 1-\gamma; 1-\beta\delta; \frac{x_0}{x_1}) = 0 .
\end{aligned} \tag{72}$$

The parameter C for each universality class is determined by adjusting C until a minimum total deviation of Γ/Γ' , R_x and ξ_0/ξ_0' from

their respective experimental values is obtained. In this exercise, we are also interested to see whether the best fit to each universal amplitude ratio would yield a consistent value of C . The parameter C does not simply assume any arbitrary values. The range of C that we can adjust lies between -1 and $(\delta-1)$ (see Eq. (52)). If C is less than -1 , we obtain a negative value of x_0/x_1 which yields complex values of the universal amplitude ratios. And, if C is greater than $(\delta-1)$, we obtain an unphysical value of $x_0/x_1 > 1$. $x_0/x_1 > 1$ means that the pseudospinodal curve lies above the coexistence curve. Thus, we find for the (3,1), (3,2), and the (3,3) model systems the allowed range of C is $-1 < C \leq 3.82$; and, for the (2,1) model the range is $-1 < C \leq 14$. The best value of the parameter C obtained for each universality class is presented in the next section.

Appendix A contains the computer program which we have written to find C and numerically calculate x_0/x_1 , $\tilde{h}(x)$ and the universal amplitude ratios.

B. Results:

1. Universal Amplitude Ratios:

Tables 3 to 6 list the predicted values of Γ/Γ' , R_X and ξ_0/ξ_0' calculated, for all the universality classes, using several different values of C . For completeness, we also include the value of x_0/x_1 , obtained for each C . Notice that we have only used Γ/Γ' and R_X to determine the C 's for all the universality classes except the (3,1). The reason is published experimental results of ξ_0/ξ_0' for the (3,2) and (3,3) model systems are not available; and, as far as we know, the exact value of ξ_0/ξ_0' for the two-dimensional Ising model has never been calculated.

Table 3: (3,1) Model System ($\beta=0.324$ and $\delta=4.82$):
Values of Γ/Γ' , R_x and ξ_0/ξ_0' obtained
using several different values of C . The
experimental values used are given in
brackets.

C	x_0/x_1	Γ/Γ' (4.9) ^a	R_x (1.69) ^a	ξ_0/ξ_0' (2.22) ^b
-0.9	0.030	5.21	1.570	0.63
-0.5	0.124	4.84	1.378	1.47
-0.3	0.163	4.85	1.367	1.79
-0.2	0.182	4.85	1.367	1.94
-0.1	0.200	4.85	1.366	2.09
0.0	0.218	4.85	1.365	2.23
0.1	0.236	4.85	1.365	2.37
0.2	0.253	4.85	1.365	2.51
0.3	0.270	4.84	1.365	2.64
0.5	0.303	4.82	1.365	2.90
1.0	0.384	4.71	1.367	3.53

^a Reference 25.

^b Reference 34.

Table 4. (3,2) Model System ($\beta=0.346$ and $\delta=4.81$): Values of r/r' and R obtained using several different values of C . The experimental values used are given in brackets.

C	x_0/x_1	r/r' (2.67) ^a	R_x (1.29) ^a
0.0	0.213	5.59	1.59
1.0	0.364	5.38	1.58
2.0	0.515	4.73	1.50
3.0	0.704	3.55	1.32
3.1	0.728	3.39	1.30
3.25	0.767	3.11	1.25
3.4	0.811	2.78	1.21
3.44	0.824	2.68	1.19
3.5	0.844	2.53	1.17
3.6	0.882	2.22	1.13
3.65	0.903	2.04	1.11
3.7	0.926	1.82	1.08

^a Reference 34.

Table 5. (3,3) Model System ($\beta=0.362$ and $\delta=4.82$): Values of Γ/Γ' and R_x obtained using several different values of C . The experimental values used are given in brackets.

C	x_0/x_1	Γ/Γ' (3.8) ^a	R_x (1.65) ^a
0.0	0.204	6.60	1.88
1.0	0.340	6.29	1.84
2.0	0.480	5.42	1.72
2.4	0.544	4.91	1.64
2.6	0.580	4.61	1.59
2.8	0.619	4.27	1.53
3.0	0.662	3.90	1.47
3.05	0.674	3.79	1.45
3.1	0.686	3.69	1.43
3.2	0.712	3.46	1.39
3.3	0.741	3.21	1.35
3.4	0.773	2.94	1.30

^a These are the average of the experimental results of Γ/Γ' and R_x displayed in Table 9.

Table 6. (2,1) Model ($\beta=0.125$ and $\delta=15$): Values of Γ/Γ' and R_x obtained for several different values of x_0 . The values in brackets are exact results obtained from Ref. 33.

C	x_0/x_1	Γ/Γ' (37.6936...)	R_x (6.78)
-0.9	0.0272	39.11	3.66
-0.5	0.0783	34.27	2.88
-0.3	0.0956	34.12	2.84
0	0.1175	34.09	2.83
1	0.1735	33.95	2.86
3	0.2563	32.47	2.89
14	0.9808	0.75	1.04

For the universality classes (3,1) and (3,3), there exists a number of published experimental values of Γ/Γ' , R_χ and ξ_0/ξ_0' , which we may use in determining the C's. The problem of choosing the right experimental values then arises; indeed, we do not know which are the most accurate and thus the best values to use. In this situation, we have chosen the most recent published experimental values. If, however, up-to-date values are not available, we have taken the average of all the published experimental results. We should also stress that all the experimental results of Γ/Γ' , R_χ and ξ_0/ξ_0' , which we have used in obtaining C, are not results of direct experimental measurements. These values were calculated using the parameters obtained from fitting various PVT data to either the MSLG or linear model equation of state.^{33,34} Thus, the accuracy of these values depends on the equation of state analysis. Hence, the values of C we obtained in this work are only approximate. However, if a consistent value of C is obtained, then our approach of determining C is very reasonable. Of course, results of direct experimental determinations of the universal amplitude ratios are desirable in order to obtain a precise value of C for each universality class.

As can be seen from the tables, the best choice of C we obtained for each model system is as follows: $C = 0.0 \pm 0.3$ for the (3,1), $C = 3.44 \pm 0.30$ for the (3,2), $C = 3.05 \pm 0.60$ for the (3,3), and $C = -0.9$ for the (2,1) model. The approximate error in each C can be estimated by inspection of the respective table. Examination of all tables shows that the best fit to each universal amplitude ratio does indeed produce a fairly consistent value of C that is within the range of the experimental uncertainties. This is nearly true for all classes of systems except the (2,1). For this model, we fail to get any reasonable

value of R_χ for $-1 < C \leq 14$; the best we could obtain is as large as 45% from its exact value. This suggests that our equation of state may not be a good representation of the two-dimensional Ising model.

Using the value of C we have determined for each universality class, we next calculate other universal amplitude ratios. Our results, together with other available theoretical results and data, are displayed in Tables 7 to 10. We should point out that since $C = 0$ is the best choice of C for the (3,1) model system, the results we obtained for this model, which are given in Table 7, are also the results obtained by Sorensen and Semon.¹⁵ Inspection of this table shows excellent agreement between our predictions and those of data and other theoretical estimates. For the (3,2) model, other theoretical results are not available for comparison except the ϵ -expansion result for A/A' . Our estimate of A/A' is about 60% larger than the experimental and the ϵ -expansion results. The results we obtained for the universality class (3,3) are presented in Table 9. Our predicted value of Γ/Γ' is favorably close in comparison to other experimental data; similarly, the value of R_χ we estimated is also very comparable to other theoretical results and data. However, our prediction of A/A' for this model disagrees completely with data and other theoretical estimates.

Since our equation for Γ/Γ' works very well for the (3,2), (3,3) and the (2,1) model, we expect that the ϵ_0/ϵ_0' relation should work reasonably well too for these models. Hence, even though no data and other theoretical results are available for comparison, we feel that our results of ϵ_0/ϵ_0' are reasonable estimates for these classes of systems.

Sorensen and Semon¹⁵ observed that the value of A/A' for the universality class (3,1) is extremely sensitive to the values of β and δ .

Table 7. (3,1) Model: $\beta=0.324\pm0.006$,
 $\delta=4.82\pm0.06$, and $C=0.0\pm0.3$.
Comparison of universal amplitude ratios.

Universal Amplitude Ratio	Our Theory	Data	Other Theoretical Results	
			Series Ising ^a	ϵ -expansion ^a
Γ/Γ'	4.86 ± 0.40	4.5 ^b (Xe) 4.9 ^c (CO ₂)	5.03	4.80
R_X	1.4 ± 0.1	1.4 ^b (Xe) 1.69 ^c (CO ₂)	1.75	1.6
ξ_0/ξ_0'	2.23 ± 0.07	2.04 ^b (Xe) 2.22 ^b (CO ₂)	1.96	--
A/A'	0.58 *	0.44 (He ³) ^a 0.63 (Xe) ^a	0.51	0.55

* This is the value of A/A' obtained for $\beta=0.324$ and $\delta=4.82$.

^a Reference 24 and 33.

^b Reference 34.

^c Reference 25.

Table 8. (3,2) Model: $\beta=0.346\pm0.009$,
 $\delta=4.81\pm0.08$, and $C=3.44\pm0.30$.
Comparison of universal amplitude ratios.

Universal Amplitude Ratio	Our Theory	Data	Other Theoretical Results	
			Series Ising ^a	ϵ -expansion ^a
Γ/Γ'	2.68 ± 0.30	2.67^b (He ⁴ λ -point)	--	--
R_χ	1.19 ± 0.10	1.29^b (He ⁴ λ -point)	--	--
ξ_0/ξ_0'	7.3 ± 0.3	--	--	--
A/A'	1.74^*	1.07^a (He ⁴ λ -point)	--	1.03

* This is the value of A/A' obtained for $\beta=0.346$ and $\delta=4.81$.

^a Reference 33.

^b Reference 34.

Table 9. (3,3) Model: $\beta=0.362\pm0.012$,
 $\delta=4.82\pm0.12$, and $C=3.05\pm0.60$.
Comparison of universal amplitude ratios.

Universal Amplitude Ratio	Our Theory	Data	Other Theoretical Results	
			Series Ising ^a	ϵ -expansion ^a
Γ/Γ'	3.79 ± 0.20	3.7^a (Eu0) 3.9^a (Ni)	--	--
R_χ	1.45 ± 0.14	1.6^a (Eu0) 1.7^a (Ni)	1.23	1.33
ξ_0/ξ_0'	6.22 ± 0.10	--	--	--
A/A'	26.16 *	1.6^a (Eu0) 2.0^a (Ni)	1.52	1.36

* This is the value of A/A' for $\beta=0.362$ and $\delta=4.82$.

^a Reference 33.

Table 10. (2,1) Model: $\beta=0.125$, $\delta=15$,
and $C=-0.9$. Comparison of
universal amplitude ratios.

Universal Amplitude Ratio	Our Theory	Exact Results
Γ/Γ'	39.11	37.6936...*
R_χ	3.66	6.78 *
ξ_0/ξ_0'	2.68	--
A/A'	--	1

* Reference 33.

They found a large variation in A/A' when they let β vary by ± 0.006 around 0.324, and δ by ± 0.06 around 4.82. We also observe a similar behavior in A/A' for the universality class (3,2). If we let both $\beta = 0.346$ and $\delta = 4.81$ vary by ± 0.009 and ± 0.08 , respectively, we find A/A' has a minimum value of 0.75 for the minimum $\beta(0.337)$ and $\delta(4.73)$, and a maximum value of 3.04 for the maximum $\beta(0.355)$ and $\delta(4.89)$. When we fix β at 0.346 and vary δ , we get a minimum A/A' of 0.93 and a maximum of 2.01. The variation in A/A' is by far the worst for the universality class (3,3). A/A' varies very rapidly and extremely large with respect to the variation in β when δ is held fixed. For example, if we fix β at 0.362 and vary δ by ± 0.12 around 4.82, A/A' becomes as large as 124.7 when $\delta = 4.83$. A/A' has a value of 2.26 for the minimum $\delta(4.7)$, and a value of 3.08 for the maximum $\delta(4.94)$.

Since A/A' is extremely sensitive to β and δ , the values of A/A' we predicted for all the model systems are therefore not very reliable. It may be just a coincidence that we get reasonably good estimate of A/A' for the (3,1) model. The strange behavior of A/A' may be due to the fact that our equation is not analytic at $x = 0$ and $x = \infty$. The analyticity of our equation of state will be further discussed in the next section.

2. Comparison to Other Equations of State:

In this section, we compare our equation of state with the equation of Milosëvić and Stanley³⁸ for the (3,3) model, and with the equations of Gaunt and Domb³ for the three- and two-dimensional Ising models. There is no equation for the universality class (3,2) available for comparison.

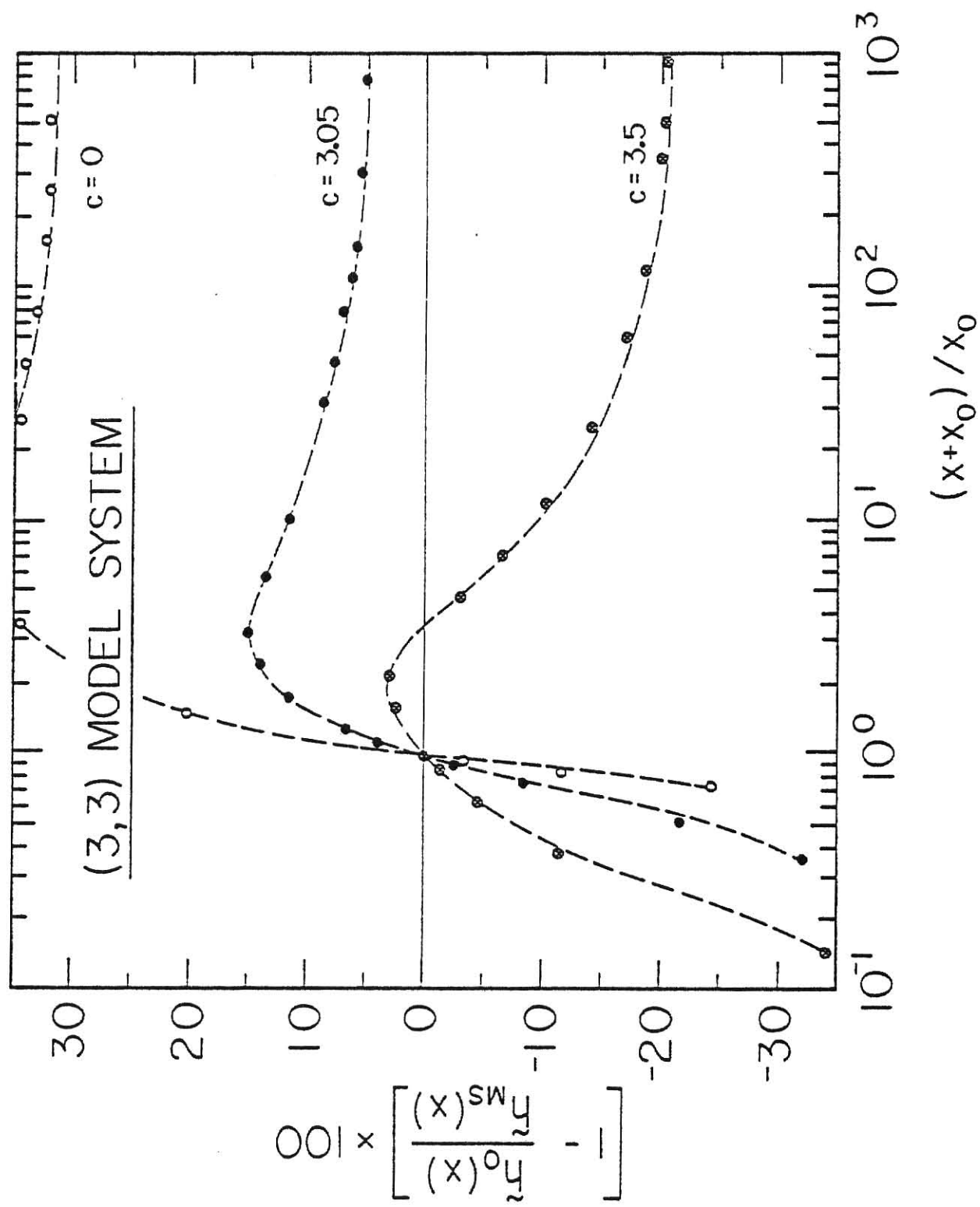
Milosëvić and Stanley³⁸ have used the low-temperature series method to derive an equation of state for the three-dimensional Heisenberg

model. In their paper, they have also compared the equation with experimental data of CrBr_3 . The equation describes the data quite well for all values of x ; on the average it deviates within less than 15% from the experimental data. For this reason, we have used their equation for comparison to ours. Figure 7 shows the deviation plot of our equation from theirs for three different values of the adjustable parameter C . In graphing the deviation plot, we have normalized our equation ($\tilde{h}_0(x) = h_0(x)/h_0(0)$) and their equation ($\tilde{h}_{\text{MS}}(x) = h_{\text{MS}}(x)/h_{\text{MS}}(0)$) such that they both match at $x = -x_0$ and $x = 0$ for any value of C . In order to be consistent, we have also used their values of $\beta = 0.385$ and $\delta = 4.71$. Figure 7 shows that in the region $x \leq 0$ all the three curves deviate by more than 20% from the equation of Milošević and Stanley; the deviation is the worst for the $C = 0$ curve. The large deviation around $x = 0$ is due to the fact that our equation is not analytic at $x = 0$. However, in the region of large x , the $C = 3.05$ curve approaches their equation within less than 5% deviation. Such a plot like Figure 7 actually provides another possible method of obtaining the best value of C . From Figure 7, it is obvious that the $C = 3.05$ curve has the least overall deviation from the equation of Milošević and Stanley; and it is well within a typical experimental error obtained by them, especially in the region of large x . Indeed, $C = 3.05$ is a very reasonable choice for the (3,3) model system.

In order to see how well our equation compares with other equations of state for the (3,1) model system, we have used the equation of Gaunt and Domb³ for the three-dimensional Ising model derived from the high-temperature series expansion. Again, to obtain consistency in our comparison, we have adopted the same $\beta(0.3125)$ and $\delta(5.0)$ as were used

Figure 7

(3,3) Model System: percent deviation plot of our equation of state, for three different values of C , from the equation of Milosëvić and Stanley. $\tilde{h}_0(x) = h_0(x)/h_0(0)$ is our normalized equation and $\tilde{h}_{MS}(x) = h_{MS}(x)/h_{MS}(0)$ is the normalized equation of Milosëvić and Stanley.



by them. The deviation plot similar to Figure 7 for this model is shown in Figure 8. Inspection of Figure 8 shows that the $C = -0.9$ curve has the least overall percent deviation for all range of x , implying that $C = -0.9$ is the best choice of the parameter C for the (3,1) model. This contradicts the results we obtained from the previous section. It turns out that this procedure of determining the best C is not a very reliable one for this model system since the equation of Gaunt and Domb does not compare very well with fluid data in the region of large x . Their equation underestimates the data (Xe , CO_2 and He^4) by more than 20%.³ On the other hand, our equation with $C = 0$ shows excellent agreement with data (Xe and He^4)¹⁵ in this region. If this is the case, then from Figure 8 we indeed find that $C = 0$ is actually the best choice of C for the (3,1) model.

In Figure 9, we compare our equation ($C = -0.9$) with the equation of Gaunt and Domb³ for the two-dimensional Ising model. Inspection of Figure 9 and the results we obtained from the preceeding section shows that our equation of state does not work very well for the universality class (2,1).

From the results of this section and the last section, we conclude that our equation of state is a reasonably good representation of the (3,1) model system using $C = 0$ and of the (3,3) model system using $C = 3.05$. Even though we have not compared our equation to other theoretical equations of state for the (3,2) model, we feel that our equation with $C = 3.44$ also provides a reasonable description of this class of systems. The results of the previous section supports this.

C. Analyticity of Equation of State:

Inspection of Figure 9 shows that there exists an inflection of

Figure 8

(3,1) Model System: percent deviation plot of our equation of state, for three different values of C , from the equation of Gaunt and Domb for the three-dimensional Ising model. $\hat{h}_0(x) = h_0(x)/h_0(0)$ is our normalized equation and $\hat{h}_{GD}(x) = h_{GD}(x)/h_{GD}(0)$ is the normalized equation of Gaunt and Domb.

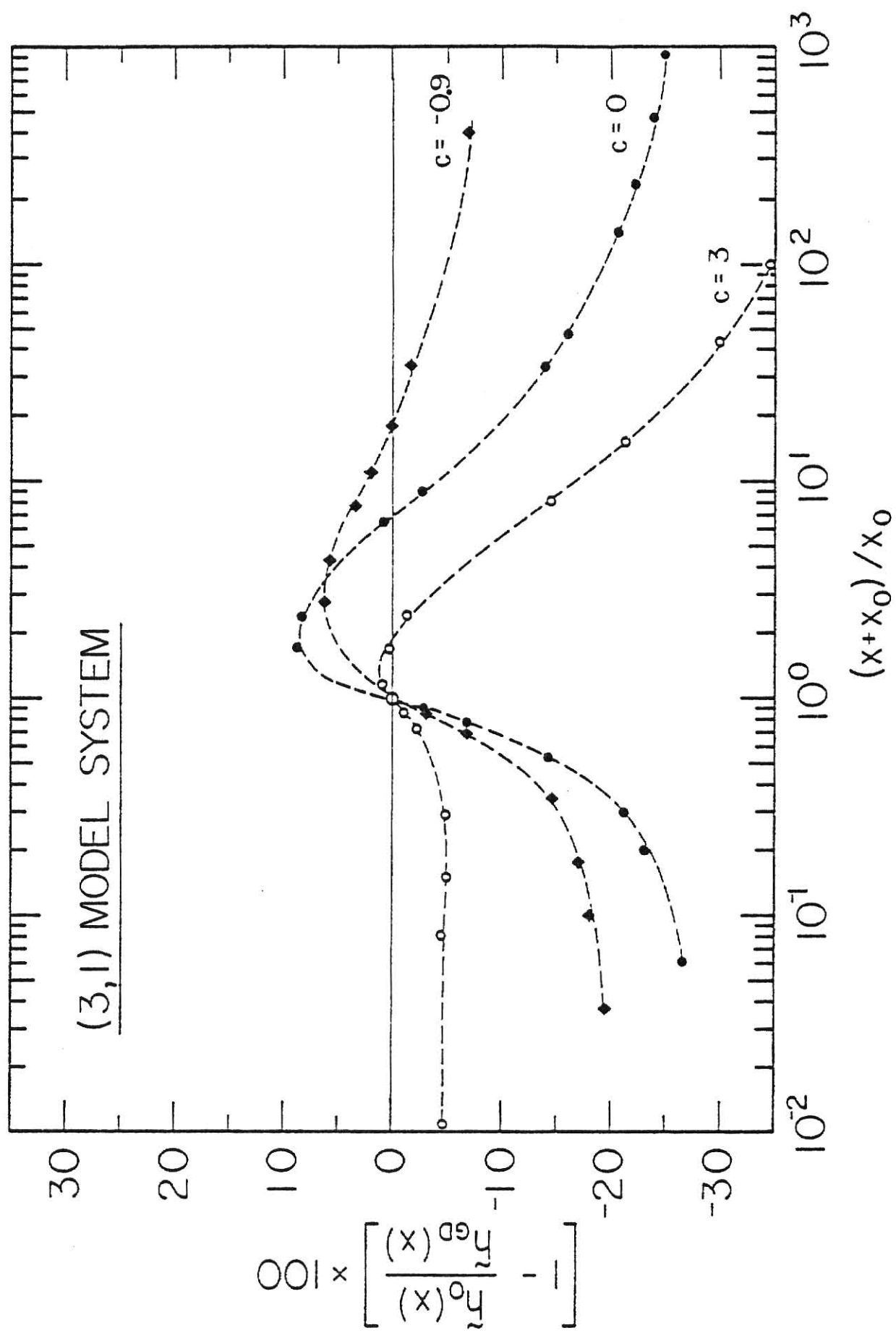
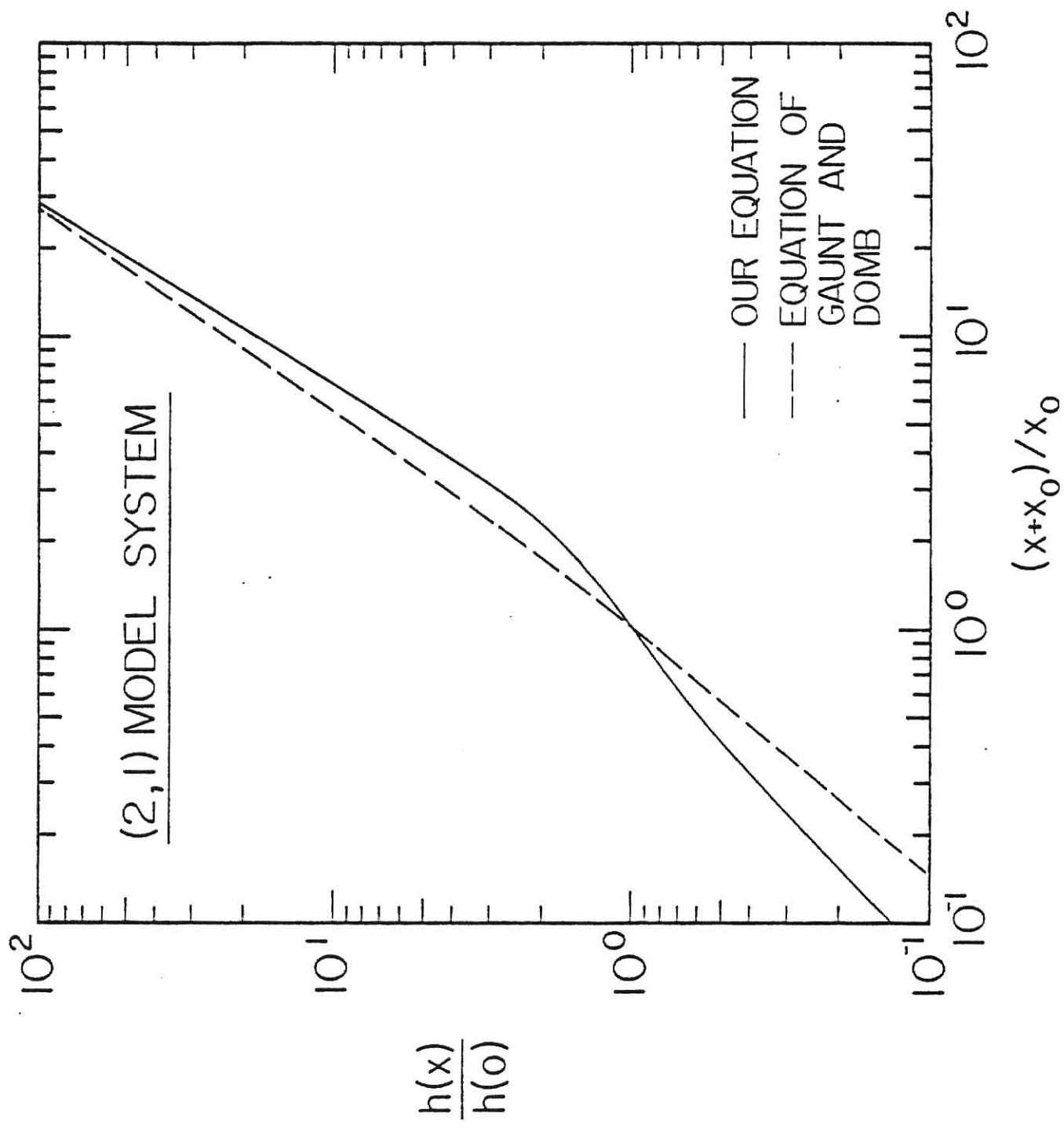


Figure 9

(2,1) Model System: comparison of our equation of state (using $\beta = 0.125$, $\delta = 15$, and $C = -0.9$) to the equation of Gaunt and Domb for the two-dimensional Ising model.



the curve $h(x)/h(0)$ at $(x+x_0)/x_0 = 1$. Similar inflections are also observed when graphs of $h(x)/h(0)$ versus $(x+x_0)/x_0$ are plotted for the other model systems. This particular feature of the curve $h(x)/h(0)$ is due to the nonanalyticity in the equation of state Eq. (52).

As predicted by Chu et al.,¹⁰ the equation of state given by Eq. (52) and (71) is analytic in $\Delta\rho^*$ and ΔT^* everywhere except on the critical isochore ($\Delta\rho^* = 0$) and critical isotherm ($\Delta T^* = 0$). The nonanalyticity in temperature on the critical isotherm is due to the homogeneous $x|x|^{\beta\delta-1}$ term, which makes the equation of state have only one continuous derivative in temperature at $x = 0$ for $\beta \sim \frac{1}{3}$ and $\delta \sim 4.8$, and also for $\beta = 1/8$ and $\delta = 15$. However, the latter, as in the case of the two-dimensional Ising model, diverges faster as $x \rightarrow 0$. The nonanalyticity in density on the critical isochore can be seen by examining the power series for $\Delta\mu^*$ as $x \rightarrow \infty$ ($\Delta\rho^* \rightarrow 0$). In this case, $h(x)$ is represented by Eq. (71b), and power series of terms $x^{\gamma-n}$, $x^{\gamma-1-n}$, with $n = 0, 1, 2, \dots$. Using $x = \Delta T^*/(\Delta\rho^*)^{1/\beta}$ in these series, we find

$$\Delta\mu^* \approx \Delta\rho^* \sum_{n=0}^{\infty} f_n(\Delta T^*) \Delta\rho^{*n/\beta} \quad (73)$$

as $x \rightarrow \infty$ (i.e. $\Delta\rho^* \rightarrow 0$). For $\beta \sim \frac{1}{3}$, $\Delta\mu^*$ has four continuous derivatives in density on the critical isochore, but is not analytic there. On the other hand, as pointed out by Sorensen and Semon¹⁵ in their paper, $\Delta\mu^*$ is smooth on both the critical isochore and isotherm, thus satisfying Griffiths' original intent. Griffiths¹¹ clearly states that the requirement of analyticity follows "neither from the thermodynamic requirements nor (excluding special cases) from statistical calculations and merely reflects the usual aesthetic desire in theoretical science to use functions 'as smooth as possible'." Of course, it will be ideal and most desirable to have an equation of state that is analytic.

We should point out that it is possible to make the equation of state, Eq. (52), analytic in temperature on the critical isotherm. This is achieved by letting $C = \delta - 1$ in accordance with what the spherical model would predict. A quick look at Eq. (52) and (71) shows that this choice of C eliminates the term $x|x|^{\beta\delta-1}$. However, we find that this improved analyticity in the equation of state poorly predicts the universal amplitude ratios when compared to data and other theoretical results. For example, we obtain $r/r' = 0.98$ and $R_\chi = 1.02$ for universality class (3,2); and $r/r' = 1.47$ and $R_\chi = 1.02$ for the (3,3) class. Hence, as far as our theoretical approach is concerned, we find that the equation of state which is nonanalytic in temperature on the critical isotherm works better in predicting the universal amplitude ratios than the analytic one.

In any event, as discussed above, the nonanalyticity is to be expected from the approach and comes from assuming that the pseudospinodal has the same exponents as the coexistence curve--an assumption required by the scaling hypothesis¹⁰ and supported by data.^{9,10,12-14}

Chapter 5

EVIDENCE FOR THE UNIVERSALITY OF THE PSEUDOSPINODAL

In Chapter 3, we have seen that generalization of Eq. (54) (i.e. the relation for Γ/Γ'), to obtain other universal amplitude ratios for other parameters diverging on the compressibility pseudospinodal, does not work for A/A' . In the preceding chapter, we have also found that the equation of state, derived either from Benedek's pseudospinodal assumption ($C = 0$) or the revised assumption ($C \neq 0$), is unable to predict reliable values of A/A' . Alternatively, we could obtain an equation of state from the specific heat pseudospinodal, i.e.,

$$C_V^*/T = A\{(T-T_S(\rho))/T_C\}^{-\alpha} \quad (73)$$

A quick and trivial derivation, which involves the following relations

$$\begin{aligned} a''(x) &= A(x + x_S)^{-\alpha} \\ h(x) &= (\delta + 1) a(x) - \frac{x}{\beta} a'(x) \end{aligned} \quad (74)$$

where $x_S = |\Delta\rho^*|^{-1/\beta} \{(T_C - T_S(\rho))/T_C\}$ is the value of x on the specific heat pseudospinodal, yields an equation of state that is different in form from Eq. (52). We find that the equation does not satisfy most of Griffiths¹¹ requirements, nor agrees with data, and does not reduce properly to the van der Waals equation in the classical limit.

The first two results quoted above for A/A' indicate that the

specific heat does not diverge on the compressibility pseudospinodal. The failure to obtain a reasonable equation of state from the specific heat pseudospinodal suggests that the pseudospinodal assumption (both Benedek's form and the revised form) may not correctly represent the approximate behavior of the specific heat along the off-critical isochores.

For these reasons, in this chapter we have used available experimental evidence to see if specific heat and other thermodynamic and transport properties of systems within a certain universality class diverge on the same or universal pseudospinodal curve.⁴³ To test the universality of the pseudospinodal, we have attempted to use all available experimental results^{10,12-14} of binary-fluid systems specifically designed to test the pseudospinodal assumption. We have also analyzed experimental data of liquid-gas systems not specifically designed for this problem but with sufficient off-critical isochore data to allow for our analysis. Surprisingly, such data are very rare. We have used specific heat data for He⁴³⁹ and CO₂,⁴⁰ thermal diffusivity data for CO₂,⁴¹ and PVT data for He⁴.¹³ The PVT data were used to graphically obtain inverse isothermal compressibility data of He⁴ along the off-critical isochores.

In analyzing each set of data, a background term of the form $B + D\Delta\rho^* + E\Delta T^*$, where B, D and E are constants, was used to correct for nonsingular behavior. A very detailed discussion of this background term is given in Ref. 39. The backgrounds were found both graphically and using a fitting procedure. Both methods were found to be consistent. The data along each isochore were then fit with a least-squares method to the original Benedek assumption, i.e.,

$$\begin{aligned}
 X &= X_0 \{ (T - T_S(\rho)) / T_C \}^{-X} \\
 &= X_0 (\Delta T^* + \Delta T_S^*)^{-X}
 \end{aligned}$$

by varying ΔT_S^* , where $\Delta T_S^* = (T_C - T_S(\rho)) / T_C$, to obtain the best fit. The results of this fitting procedure for all four sets of data are presented in Tables 11 to 14. Inspection of all tables shows that fits to all isochores yielded, within error, the same value of X_0 and x obtained on the critical isochore. Thus, it is important to stress that the consistency of the pseudospinodal is well verified. For completeness, the values of ΔT_S^* obtained along each isochore is also given in the tables.

To determine the amplitude B_S and the exponent β^+ (i.e. the shape of the pseudospinodal curve), the values of ΔT_S^* obtained were then fit to Eq. (38), i.e.,

$$\Delta T_S^* = B_S \{ (T_C - T_S(\rho)) / T_C \}^{\beta^+}.$$

When the pseudospinodal curve was found not to be symmetric, the following form of Eq. (38),

$$\frac{1}{2} \left(\frac{\rho' - \rho''}{\rho_C} \right) = B_S \{ (T_C - T_S(\rho)) / T_C \}^{\beta^+},$$

was used. In the above equation, ρ' and ρ'' are densities or concentrations of the two phases. Our results along with earlier published pseudospinodal curves are displayed in Table 15. Inspection of Table 15 shows that there is a small but persistent tendency for $\beta^+ \geq \beta$ in nearly all cases. This is especially true for both sets of specific heat data. In fact, the values of β^+ obtained from these two sets of data are extraordinarily large compared to other β^+ 's. The data for CO_2 have essentially the mean field value of $\beta^+ \approx \frac{1}{2}$.

Table 11. Specific heat of He⁴: Results of fitting the data along each isochore to $C_V^*/T = A(\Delta T^* + \Delta T_S^*)^{-\alpha}$.

ρ (g/cm. ³)	A	α	ΔT_S^*
$\rho_c = 0.06958$	1.197	0.127	0
0.0694	1.245	0.132	1.95×10^{-5}
0.0766	1.220	0.126	2.14×10^{-3}
0.0623	1.313	0.123	1.85×10^{-3}
0.0660	1.280	0.128	4.05×10^{-4}
0.0732	1.262	0.124	5.97×10^{-4}
0.0805	1.211	0.128	8.30×10^{-3}

Table 12. Specific heat of CO₂: Results of fitting the data along each isochore to $C_v^*/T = A(\Delta T^* + \Delta T_S^*)^{-\alpha}$.

ρ (g/cm. ³)	A	α	ΔT_S^*
$\rho_c = 0.467$	0.127	0.124	0
0.483	0.127	0.129	1.0×10^{-3}
0.513	0.127	0.127	2.0×10^{-3}
0.570	0.129	0.125	1.3×10^{-2}
0.606	0.128	0.124	1.8×10^{-2}
0.629	0.127	0.126	2.6×10^{-2}

Table 13. Thermal conductivity of CO₂:
Results of fitting the data
along each isochore to
 $\lambda = \lambda_0 (\Delta T^* + \Delta T_S^*)^{-\kappa}$.

ρ (amagat)	λ_0	κ	ΔT_S^*
$\rho_c = 236$	0.074	0.60	0
200	0.082	0.60	4.7×10^{-3}
210	0.083	0.60	2.3×10^{-3}
230	0.083	0.59	1.0×10^{-4}
220	0.081	0.60	7.0×10^{-4}
240	0.081	0.59	0
250	0.079	0.58	1.0×10^{-4}
260	0.079	0.60	1.5×10^{-3}
270	0.077	0.57	3.6×10^{-3}

Table 14. Inverse isothermal compressibility of He⁴: Results of fitting the data along each isochore to $(K_T^* \rho^*)^{-1} = 1/\Gamma(\Delta T^* + \Delta T_S^*)^\gamma$.

ρ (g/cm. ³)	Γ^{-1}	γ	ΔT_S^*
$\rho_c=0.069$	1.01×10^4	1.155	0
0.040	1.1×10^4	1.17	5.5×10^{-2}
0.051	9.94×10^3	1.18	2.3×10^{-2}
0.0566	8.6×10^3	1.15	1.0×10^{-2}
0.064	8.56×10^{-3}	1.13	1.0×10^{-3}
0.072	1.1×10^4	1.14	5.0×10^{-4}
0.075	1.2×10^4	1.12	1.5×10^{-3}
0.082	1.2×10^4	1.12	2.0×10^{-2}
0.078	1.8×10^4	1.19	4.0×10^{-3}

Table 15. A list of pseudospinodal and coexistence curves obtained from either our data analysis or the analysis in the published work.

Thermodynamic or transport property and system	Coexistence Curve	Pseudospinodal Curve
Diffusivity and correlation length of isobutyric acid in H ₂ O ^a	$\frac{\rho' - \rho''}{\rho_C} = 5.82 \Delta T^{*1/3}$	$\frac{\rho' - \rho''}{\rho_C} = 4.42 \Delta T^{*1/3}_S$
Viscosity of isobutyric acid in H ₂ O ^b	$\frac{\rho' - \rho''}{\rho_C} = 6.78 \Delta T^{*0.36}$	$\frac{\rho' - \rho''}{\rho_C} = 4.69 \Delta T^{*0.37}_S$
Correlation length of polystyrene-cyclohexane	$\frac{\rho' - \rho''}{\rho_C} = 14.68 \Delta T^{*0.37}$	$\frac{\rho' - \rho''}{\rho_C} = 10.24 \Delta T^{*0.38}_S$
Osmotic compressibility and correlation length of polystyrene in diethyl malonate	$\frac{ \rho - \rho_C }{\rho_C} = 0.295 \Delta T^{*1/3}$	$\frac{ \rho - \rho_C }{\rho_C} = 0.25 \Delta T^{*0.35}_S$
Specific heat of He ⁴ ^e	$\frac{ \rho - \rho_C }{\rho_C} = 1.57 \Delta T^{*0.3724}$	$\frac{\rho' - \rho''}{\rho_C} = 2.63 \Delta T^{*0.41}_S$
Specific heat of CO ₂ ^f	$\frac{ \rho - \rho_C }{\rho_C} = 1.54 \Delta T^{*0.3486} \text{ g}$	$\frac{ \rho - \rho_C }{\rho_C} = 2.07 \Delta T^{*0.495}_S$
Thermal conductivity of CO ₂ ^h	$\frac{ \rho - \rho_C }{\rho_C} = 1.54 \Delta T^{*0.3486} \text{ g}$	$\frac{\rho' - \rho''}{\rho_C} = 1.9 \Delta T^{*0.34}_S$

Table 15. A list of pseudospinodal and coexistence curves obtained from either our data analysis or the analysis in the published work (continued).

Thermodynamic or transport property and systems	Coexistence Curve	Pseudospinodal Curve
Inverse isothermal compressibility of He^4	$\frac{\rho' - \rho''}{\rho_C} = 2.77 \Delta T^* 0.35$	$\frac{\rho' - \rho''}{\rho_C} = 1.84 \Delta T_S^* 0.37$
a Reference 10.	f Reference 40.	
b Reference 13.	g Reference 34.	
c Reference 12.	h Reference 41.	
d Reference 14.	i Reference 42.	
e Reference 39.		

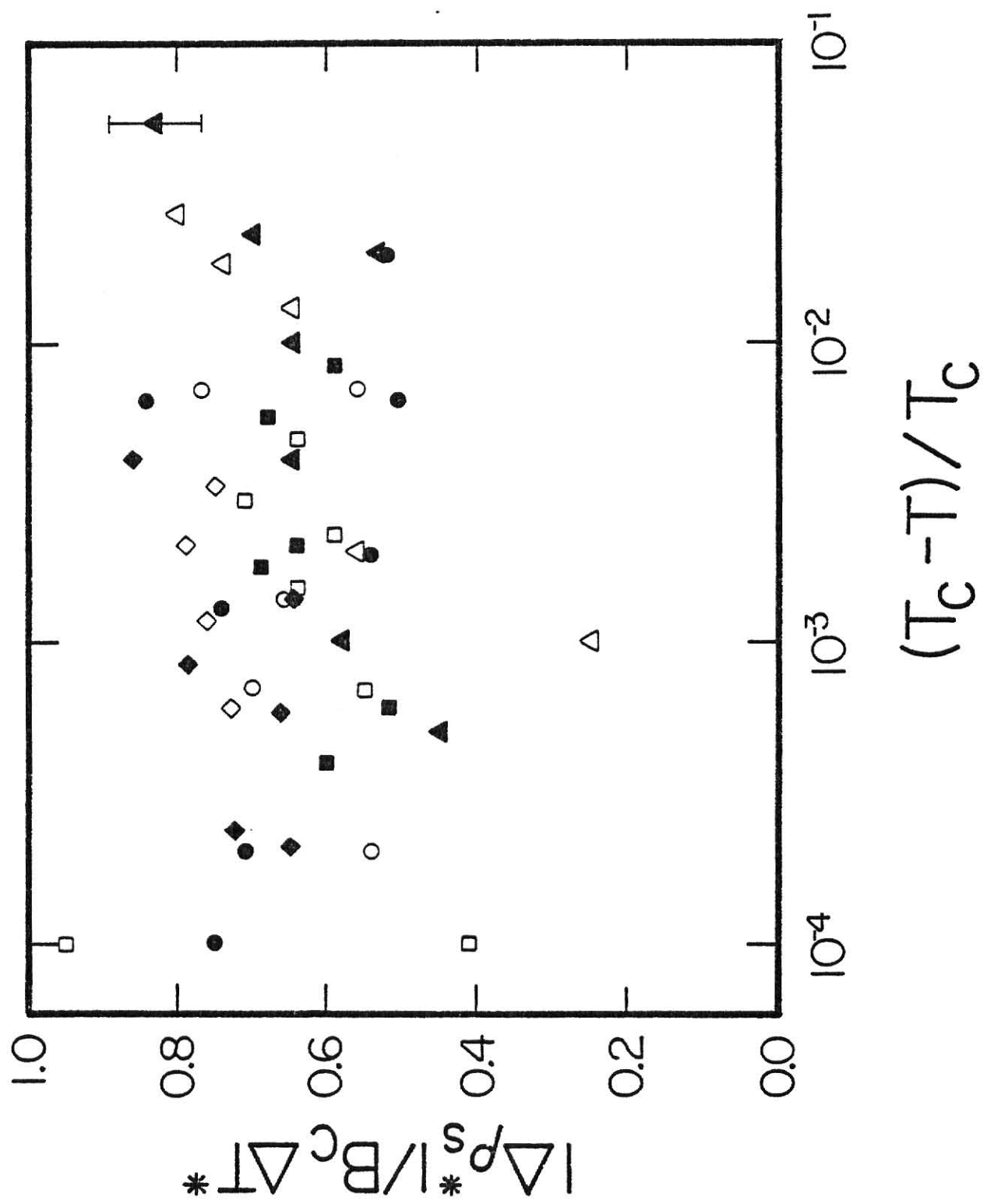
To compare these various pseudospinodals, we normalized relative to the coexistence curve of the fluid. However, some ambiguity in coexistence curves arises. When possible, we used the coexistence curve that was presented with or could be obtained from the data used to find the pseudospinodal. Otherwise, the best literature value was used. The ambiguity is usually only a few percent. Thus, along any given isotherm ΔT^* , we divide a given data value $|\Delta \rho_S^*| = (\rho_S - \rho_C)/\rho_C$ on the pseudospinodal curve by $\Delta \rho^* = (\rho - \rho_C)/\rho_C = B_C \Delta T^{*\beta}$, the value on the coexistence curve. This method of normalization is preferable to simply dividing the pseudospinodal by B_C because of statistical correlations between B_C and β .

Figure 10 is a plot of normalized pseudospinodal curve data, $|\Delta \rho_S^*|/B_C \Delta T^{*\beta}$, versus reduced temperature ΔT^* . To within the large scatter of the data, the pseudospinodal curves for the various substances and properties do display universal behavior. This possible universality indicates that the concept of the pseudospinodal may have more physical significance than we usually recognize. If $\beta = \beta^+$, then these results suggest the ratio B_S/B_C , equal to 0.66 ± 0.13 for these data, is a universal quantity. For comparison, theoretical "spinodals" predict $B_S/B_C = 0.58$ for the mean field model ($\beta = \beta^+ = \frac{1}{2}$, however), $B_S/B_C = 0.82 \pm 0.1$ for the Ising model,³ and $B_S/B_C = 0.63$ from, not surprisingly, our equation of state (with $C = 0$).

Whether the specific heat diverges on the same pseudospinodal curve as the other properties is still questionable. The results we obtained from the theoretical side clearly suggest that the specific heat diverges on the pseudospinodal different from the compressibility pseudospinodal. The rather large values of β^+ implied by the specific heat data further supports this belief. On the other hand, from Figure

FIGURE 10

Plot of pseudospinodal curve data $|\Delta\rho_S^*|$ normalized by the coexistence curve $B_C\Delta T^{*\beta}$ versus $\Delta T^* = (T-T_C)/T_C$. The symbols correspond to: \blacklozenge diffusivity and correlation length of isobutyric acid + water (Ref. 10), \diamond osmotic compressibility and correlation length of polystyrene + diethyl malonate (Ref. 14), \bullet viscosity of isobutyric acid + water (Ref. 13), \circ correlation length of polystyrene + cyclohexane (Ref. 12), \blacktriangle isothermal compressibility of He^4 (Ref. 42), \triangle specific heat of CO_2 (Ref. 40), \blacksquare specific heat of He^4 (Ref. 39), and \square thermal conductivity of CO_2 (Ref. 41). The value $|\Delta\rho^*|/B_C\Delta T^{*\beta} = 1.0$ represents the coexistence curve. A typical error bar is also shown.



10 we observe that even though β^\dagger are large, the specific heat data, when normalized with respect to the coexistence curve, do lie in the same general area as the other data points. Hence, at this point we cannot make any definite conclusion regarding the behavior of the specific heat along the off-critical isochores. In order to do this, we need more specific heat data.

As for now, we may conclude that the pseudospinodal data for both variety of properties and systems lie in the same general area of the phase diagram when normalized relative to the coexistence curve, providing evidence for the concept of a universal pseudospinodal curve, the ratio B_S/B_C being a universal amplitude ratio. However, there is some tendency for $\beta^\dagger \geq \beta$, which is especially true for the specific heat data.

Chapter 6

CONCLUSION

In this work, we have revised the Benedek pseudospinodal assumption by adding an extra or correction term. From the revised assumption, we have derived a general form of an equation of state, and subsequently, general expressions for the universal amplitude ratios.

We have found that the correction term is negligibly small for the universality class (3,1) but quite large for other classes. For the (3,1) model, we have seen that the equation of state (with $C = 0$) does not only compare better to the equation of Gaunt and Domb but fits PVT data favorably.¹⁵ Our predictions of the universal amplitude ratios Γ/Γ' , R_χ , and ξ_0/ξ_0' for this model are in good agreement with data and other theoretical results. For the (3,3) model, we have observed that the equation of state (with $C = 3.05$) compares very well to the equation of Milosëvić and Stanley; and, the estimated values of Γ/Γ' and R_χ that we have obtained agree favorably to data and other theoretical predictions. We have also discovered that using $C = 3.44$, our estimations of Γ/Γ' and R_χ for the (3,2) model are comparable to other theoretical and experimental results. Thus in this work, we have found that an addition of a correction term to the original pseudospinodal assumption improves the results on the universality classes (3,3) and (3,2). Hence, we conclude that the revised pseudospinodal assumption, which we have introduced, is a reasonable generalization of the pseudospinodal assumption since it works for all the model systems except the (2,1).

Finally, by considering data on several thermodynamic and transport properties of various liquid-gas and binary fluid systems, we have also shown evidence for the existence of a universal pseudospinodal that describes all these properties of the systems with one curve. It is possible that this universality also exists in other universality classes besides the (3,1).

Despite the fact that the equation of state derived from the pseudospinodal assumption is not analytic, we have shown that it works satisfactorily in describing the (3,1), (3,2), and the (3,3) model systems. This plus the possible existence of a universal pseudospinodal further supports the usefulness of the pseudospinodal concept in critical phenomena. As pointed out by Sorensen and Semon,¹⁵ we therefore should not discard this concept solely on the grounds of analyticity.

On the other hand, the nonanalyticity in the equation of state does pose some disadvantages. We have seen that the equation does not work very well for the universality class (2,1) because its nonanalyticity is stronger for this model since $\beta = 1/8$. It is also at least part of the problem in predicting the values of A/A' . An analytic equation of state would possibly improve these results. However, the nonanalyticity in our theoretical approach is expected since it comes from the assumption, $\beta^+ = \beta$, that we have used in deriving the equation. There may be a way of eliminating it in our equation which, at present, we have no knowledge of.

Besides the problem of nonanalyticity, another question arises from this work, that is, the question of whether the isothermal compressibility and the specific heat diverge on the same or on a different pseudospinodal. The results of this work seem to support the latter. If indeed they diverge on a different pseudospinodal curve, then it would be very

interesting to find out the behavior of the specific heat along the off-critical isochores and the form of its pseudospinodal curve. A deeper knowledge and understanding of this problem would definitely help us to explain the results we obtained in Chapter 5, and possibly would enable us to improve the A/A' calculation. Thus, we feel that a statistical mechanic and thermodynamic investigation of mechanical and thermal metastabilities is a promising extension of this work.

REFERENCES

1. H. E. Stanley, Introduction to Phase Transitions and Critical Phenomena (Oxford University Press, 1971).
2. J. V. Sengers and J. M. H. Levelt Sengers, in Progress in Liquid Physics, edited by C. A. Croxton (John Wiley and Sons, 1978).
3. D. S. Gaunt and C. Domb, J. Phys. C 3, 1442 (1970).
4. D. S. Gaunt and G. A. Baker, Jr., Phys. Rev. B 1, 1184 (1970).
5. E. Brezin, D. J. Wallace, and K. G. Wilson, Phys. Rev. Lett. 29, 591 (1972).
6. E. Brezin, D. J. Wallace, and K. G. Wilson, Phys. Rev. B 1, 232 (1973).
7. M. Vicentini-Missoni, J. M. H. Levelt Sengers, and M. S. Green, J. Res. Natl. Bur. Stan. (U.S.) 73A, 563 (1969).
8. P. Schofield, Phys. Rev. Lett. 22, 606 (1969).
9. G. B. Benedek, in "Polarisation Matière et Rayonnement, Liv're de Jubile en l'honneur du Professeur A. Kastler" (Presses Universitaires de Paris, France, 1968).
10. B. Chu, F. J. Schoenes, and M. E. Fisher, Phys. Rev. 185, 219 (1969).
11. R. B. Griffiths, Phys. Rev. 158, 176 (1967).
12. J. Kojima, N. Kuwahara, and M. Kaneko, J. Chem. Phys. 63, 333 (1975).
13. Y. Izumi and Y. Miyake, Phys. Rev. A 16, 2120 (1977).
14. K. Hamano, N. Kuwahara, and M. Kaneko, Phys. Rev. A 20, 1135 (1979).
15. C. M. Sorensen and M. D. Semon, Phys. Rev. A 21, 340 (1980).
16. B. Widom, J. Chem. Phys. 43, 3898 (1965).
17. L. D. Landau and M. E. Lifshitz, Statistical Physics (Pergamon Press Ltd., 1958).

18. A. Hankey and H. E. Stanley, Phys. Rev. B 6, 3515 (1972).
19. J. M. H. Levelt Sengers, Physica 73, 73 (1974).
20. R. B. Griffiths, Phys. Rev. Lett. 24, 1479 (1970).
21. L. P. Kadanoff, in Critical Phenomena, Proc. Intern. School of Physics, 'Enrico Fermi', Course L1, edited by M. S. Green (Academic Press, New York, 1971), p. 100.
22. L. P. Kadanoff, in Phase Transitions and Critical Phenomena, edited by C. Domb and M. S. Green (Academic Press, New York, 1976), Vol. 5A.
23. H. E. Stanley, A. Hankey, and M. H. Lee, in Critical Phenomena, Proc. Intern. School of Physics, 'Enrico Fermi', Course L1, edited by M. S. Green (Academic Press, New York, 1971), p. 237.
24. A. Aharony and P. C. Hohenberg, Phys. Rev. B 13, 3081 (1976).
25. R. Hocken and M. R. Moldover, Phys. Rev. Lett. 37, 29 (1976).
26. P. Schofield, J. D. Lister, and J. T. Ho, Phys. Rev. Lett. 23, 1098 (1969).
27. J. T. Ho and J. D. Lister, Phys. Rev. Lett. 22, 603 (1969).
28. G. A. Baker, Jr., B. G. Nickel, and D. I. Meiron, Phys. Rev. B 17, 1365 (1978).
29. J. Als-Nielsen, O. W. Dietrich, W. Kunmann, and L. Passell, Phys. Rev. Lett. 27, 741 (1971).
30. G. S. Joyce, in Phase Transitions and Critical Phenomena, edited by C. Domb and M. S. Green (Academic Press, New York, 1972), Vol. 2.
31. C. M. Sorensen, Bull. Am. Phys. Soc. 23, 339 (1978).
32. Higher Transcendental Functions, edited by A. Erdélyi (McGraw Hill, New York, 1955), Vol. I.
33. M. Barmatz, P. C. Hohenberg, and A. Kornbilit, Phys. Rev. B 12, 1947 (1975).
34. J. M. H. Levelt Sengers, W. L. Greer, and J. V. Sengers, J. Phys. Chem. Ref. Data 5, 1 (1976).
35. J. C. LeGuillon and J. Zinn-Justin, Phys. Rev. Lett. 39, 95 (1977).
36. M. E. Fisher, Rep. Prog. Phys. 30, 615 (1967).
37. C. M. Sorensen and M. D. Semon (unpublished work).

38. S. Milosević and H. E. Stanley, Phys. Rev. B 5, 2526 (1972).
39. M. R. Moldover, Phys. Rev. 182, 342 (1969).
40. K. I. Amirkhanov, N. G. Polikhronidi, R. G. Batyrova, Teploenergetika 17, 70 (1970), Thermal Engineering 101 (1970); K. I. Amirkhanov, N. G. Polikhronidi, B. G. Alibekov, and R. G. Batyrova, Teploenergetika 18, 59 (1971), Thermal Engineering, 87 (1971).
41. A. Michels, J. V. Sengers, and P. S. Van der Gulik, Physica 28, 1238 (1962).
42. D. R. Roach, Phys. Rev. 170, 213 (1968).
43. J. Osman and C. M. Sorensen, J. Chem. Phys. 73, 4142 (1980).
44. L. E. Reichl, A Modern Course in Statistical Physics (University of Texas Press, Austin, 1980).

APPENDIX A

The following is a computer program that we have written to determine C , and to numerically calculate $\tilde{h}(x) = h(x)/h(0)$ and the universal amplitude ratios. The program consists of two main programs and six subprograms. Main program A is designed such that we can determine C and numerically calculate $\tilde{h}(x)$ for each universality class. It can also be used to calculate Γ/Γ' , R_χ and ξ_0/ξ_0' . Main Program B is written to compute Γ/Γ' , R_χ , ξ_0/ξ_0' and A/A' . It is also made so that we can find the approximate range of error in each universal amplitude ratio, which is done by varying β and δ .

ILLEGIBLE DOCUMENT

**THE FOLLOWING
DOCUMENT(S) IS OF
POOR LEGIBILITY IN
THE ORIGINAL**

**THIS IS THE BEST
COPY AVAILABLE**

C MAIN PROGRAM A

```

C
REAL BETA, DELTA, G, ZO, GGP, RXI, INVZ, MU, EGGP, ERXI
1, Z, X, XX0, H, HM, K, KI, DEV, ECL, D, AB3, CL, AB1, AB2
ACCEPT *, BETA, DELTA, D, K, KF, Z, EGGP, ERXI, ECL
MU=BETA*(DELTA+1.)/D
G=BETA*(DELTA-1.)
IF (Z.NE.0.) GO TO 4
1 CALL ZERO(BETA, DELTA, K, ZO)
INVZ=1.0/ZO
GGP=((INVZ-1.0)**(G-1.0))*((INVZ*(1.0+K))-1.0)
CL=((INVZ-1.0)**(MU-1.0))*((INVZ*(1.0+K))-1.0)
RXI=(1./DELTA)*(1.0+K)*(INVZ**G)
AB1=(GGP-EGGP)/EGGP
AB2=(RXI-ERXI)/ERXI
IF (ECL.EQ.0.) GO TO 2
AB3=(CL-ECL)/ECL
2 DEV=ABS(AB1)+ABS(AB2)+ABS(AB3)
TYPE 3, K, ZO, GGP, RXI, CL, DEV
3 FORMAT(10X, F5.2, 5X, F7.5, 5X, F7.3, 5X, F6.3, 5X, F6.3, 5X, F6.3)
IF (K.GT.KF) GO TO 6
K=K+0.01
GO TO 1
4 CALL ZERO(BETA, DELTA, K, ZO)
CALL HX(BETA, DELTA, K, Z, H)
XX0=1.+(-Z/ZO)
HM=H/(1.0+K)
TYPE 5, K, ZO, XX0, HM
5 FORMAT(5X, F5.2, 5X, F8.6, 5X, F11.6, 5X, E11.4)
6 STOP
END

```

C MAIN PROGRAM B

```

C
REAL BETA, DELTA, ALPHA, G, ZO, K, AAP, GGP, RXI, INVZ, A, AP, BF
1, DF, BI, DI, MU, CL
ACCEPT *, BI, DI, BF, DF, K
BETA=BI
DELTA=DI
1 ALPHA=2.0-(BETA*(DELTA+1.0))
G=BETA*(DELTA-1.0)
MU=BETA*(DELTA+1.0)/3.
CALL ZERO(BETA, DELTA, K, ZO)
5 CALL AA(BETA, DELTA, K, A)
CALL APRIME(BETA, DELTA, K, ZO, AP)
INVZ=1.0/ZO
AAP=(INVZ**ALPHA*(ALPHA-2.0))*((A/AP)
GGP=((INVZ-1.0)**(G-1.0))*((INVZ*(1.0+K))-1.0)
CL=((INVZ-1.0)**(MU-1.0))*((INVZ*(1.0+K))-1.0)
RXI=(1./DELTA)*(1.0+K)*(INVZ**G)
TYPE 2, BETA, DELTA, ZO, AAP, GGP, RXI, CL
2 FORMAT(5X, F5.3, 5X, F4.2, 5X, F7.5, 5X, F10.5, 5X, F5.3, 5X, F5.3
1, 5X, F5.3)
DELTA=DELTA+.01
IF (DELTA.GT.DF) GO TO 3

```



```

      GO TO 1
3     TYPE 4
4     FORMAT(//)
      BETA=BETA+.001
      IF (BETA.GT.BF) GO TO 6
      DELTA=DI
      GO TO 1
6     STOP
      END

C     "ZERO" IS A SUBROUTINE THAT CALCULATES THE ZERO OF H(X).
C     E IS THE ACCURACY OF THE HYPERGEOMETRIC FUNTION EXPANSION.
C
      SUBROUTINE ZERO(B,D,C,Z)
      REAL B,D,C,Z,G,X1,X2,X3,G1,G2,G3,GTERM,CTERM,ZTERM,F1,F2,
      F3,CONST,F(2),NTERM,E,H,R
      INTEGER FACT,N,L,M
      G=B*(D-1.)
      E=.0001
      X1=1.-(B*D)
      X2=B
      X3=-G
      CALL GAMMA(X1,G1)
      CALL GAMMA(X2,G2)
      CALL GAMMA(X3,G3)
      GTERM=G1*G2/G3
      CTERM=1.-(C/(D-1.))
      R=.1
10    ZTERM=Z*(ABS(Z)**((B*D)-1.))
      F1=-G
      F2=-B*D
      F3=1.-(B*D)
      DO 40 N=1,2
      CONST=F1*F2/F3
      F(N)=1.+(CONST*Z)
      FACT=1
      DO 20 L=2,100
      FACT=FACT*L
      M=L-1
      CONST=CONST*(F1+M)*(F2+M)/(F3+M)
      NTERM=CONST*(Z**L)/FACT
      F(N)=F(N)+NTERM
      IF (NTERM.LT.E) GO TO 30
20    CONTINUE
30    F1=F1+1.0
40    CONTINUE
      H=(CTERM*GTERM*ZTERM)+F(1)+(C*F(2))
      IF (H.GT.-.0001.AND.H.LT.0.0001) GO TO 60
      IF (H.LT.0.) GO TO 50
      Z=Z+R
      GO TO 10
50    Z=Z-R
      R=R*.1
      GO TO 10
60    RETURN
      END

```

```

C      "GAMMA" IS A SUBROUTINE THAT CALCULATES THE GAMMA
C      FUNCTION OF X.
      SUBROUTINE GAMMA(X,GF)
      REAL X,GF,Y,P,GSMALL,X,B(8),Q
      DATA B/-.577191652,.988205891,-.897056937,.918206857
1      1,-.756704078,.482199394,-.193527818,.035868343/
      INTEGER N,I,U
      GF=1.0
      IF (X.LT.1.0) GO TO 20
      IF (X.LT.2.0) GO TO 40
      DO 10 N=1,100
      Y=X-N
      GF=GF*Y
      IF (Y.EQ.1.0) GO TO 20
      IF (Y.GT.1.0.AND.Y.LT.2.0) GO TO 20
10     CONTINUE
20     DO 30 I=1,100
      U=I-1.0
      P=1.0/(X+U)
      GF=GF*P
      IF ((X+U).GT.0..AND.(X+U).LT.1.) GO TO 50
      IF ((X+U).EQ.-1.) GO TO 20
30     CONTINUE
40     Y=X
      GO TO 20
50     Y=X+U+1.0
60     GSMALL=1.0
      Q=Y-1.0
      DO 70 I=1,8
      GSMALL=GSMALL+(B(I)+(Q**I))
70     CONTINUE
      GF=GF*GSMALL
80     RETURN
      END

C
C      "AA" IS A SUBROUTINE THAT CALCULATES "A".
C
      SUBROUTINE AA(B,D,K,A)
      REAL B,D,K,A,G,A1,C1,C2,C3,C4,C5,P,A2,Y,C6,C7,C8,X4,X5
1      1,A3,D2,D3,D4,D5,D6,D7,X1,X2,X3,G1,G2,G3,A4,ALPHA,A5,D8
      1,D9,A6,A7,D05,G4,G5,D1
      INTEGER FACT,I,H,J,M,L
      G=B*(D-1.0)
      ALPHA=2.-(B*(D+1.0))
      A1=0.0
      C1=-G
      IF (ALPHA.LT.0.) GO TO 21
      FACT=1
      N=-1
      DO 20 I=2,7
      N=(-1)**I
      C2=C1+(K*(I+C1))
      C3=I-(B*D)
      C4=C3-B
      FACT=FACT*I
      L=I-1
      P=1.0
      DO 10 J=1,L

```

```

      P=P*(J+C1)
10    CONTINUE
      DC5=C3+C4*FACT
      C5=N*P+C2/DC5
      A1=A1-C5
      IF (ABS(C5).LT..0001) GO TO 20
20    CONTINUE
21    FACT=2
      N=1
      DO 23 I=3,7
      N=(-1)**N
      C2=C1+(K*(I+C1))
      C3=I-(B*D)
      C4=C3-B
      FACT=FACT*I
      L=I-1
      P=1.0
      DO 22 J=1,L
      P=P*(J+C1)
22    CONTINUE
      DC5=C3+C4*FACT
      C5=N*P+C2/DC5
      A1=A1-C5
      IF (ABS(C5).LT..001) GO TO 30
23    CONTINUE
30    A2=1.0/(2.0*B*B)
      FACT=1
      N=1
      DO 40 I=1,100
      CALL GR(I,G,Y)
      C6=B+I
      C7=(2.0*B)+I
      FACT=FACT*I
      N=(-1)**I
      C8=Y*N/(C6+C7*FACT)
      A2=A2+C8
      IF (ABS(C8).LT..001) GO TO 50
40    CONTINUE
50    X4=-1.0-B
      X5=-B
      CALL GAMMA(X4,G4)
      CALL GAMMA(X5,G5)
      D1=K*(1.0+B)*G4/G5
      A3=-K*G4/(G5*((2.*B)+1.))
      FACT=1
      N=1
      P=1.0
      DO 60 J=1,100
      P=P*(J+C1)
      M=J+1
      D2=M+B
      D3=(2.0*B)+M
      N=(-1)**J
      FACT=FACT*J
      D4=N*P/(D2*D3*FACT)
      D5=D1*D4
      A3=A3-D5
      IF (ABS(D5).LT..001) GO TO 70

```

```

60      CONTINUE
70      D6=1.0/(D*B*B)
      D7=1.0-(K/(D-1.0))
      X1=1.0-(B*D)
      X2=B
      X3=-G
      CALL GAMMA(X1,G1)
      CALL GAMMA(X2,G2)
      CALL GAMMA(X3,G3)
      A4=D6*D7*G1*G2/G3
      A5=(1.+K)/(B*D*(ALPHA-2.))
      D8=1.0/(X1*(ALPHA-1.))
      D9=C1+(K*(1.0+C1))
      A6=D8*D9
      A7=((1.-G)*(C1+(K*(2.+C1))))/(ALPHA*(X1+1.))
      A=A1+A2+A3+A4+A5+A6
      IF (ALPHA.LT.0.) A=A-A7
      TYPE 99,A
99      FORMAT(10X,F10.5)
      RETURN
      END

C
C      "GN" IS A SUBROUTINE THAT COMPUTES MINUS GAMMA SUB N.
C
      SUBROUTINE GN(I,G,P)
      REAL P,G
      INTEGER I,J
      P=1.0
      DO 10 J=1,I
      P=P*((-G)+J-1.0)
10      CONTINUE
      RETURN
      END

C
C      "APRIME" IS A SUBROUTINE THAT CALCULATES "A'".
C
      SUBROUTINE APRIME(B,D,K,Z,Q)
      REAL B,D,K,Z,Q,G,ALPHA,Q1,Q2,Q3,Q4,Q5,Q6,Q7,X1,X2,X3,
      Q8,Q9,R1,R2,R3,R4,R5,R6,R7,G2,G1,G3,
      INTEGER I,J,FACT
      G=B*(D-1.0)
      ALPHA=2.0-(B*(D+1.0))
      Q1=-G
      Q=0.
      IF (ALPHA.LT.0.) GO TO 20
      FACT=1
      Q3=1.0
      DO 10 I=2,7
      Q2=Q1+(K*(I+Q1))
      J=I-1
      Q3=Q3*(J+Q1)
      FACT=FACT*I
      Q4=I-(B*D)
      Q5=Q4-B
      Q6=Z**I
      Q7=Q2*Q3*Q6/(FACT*Q4*Q5)
      Q=Q-Q7
20

```

```

10      IF (ABS(Q7).LT..0001) GO TO 40
20      CONTINUE
      FACT=2
      Q3=1.0+Q1
      DO 30 I=3,7
      Q2=Q1+(K*(I+Q1))
      J=I-1
      Q3=Q3+(J+Q1)
      FACT=FACT*I
      Q4=1-(B*D)
      Q5=Q4-B
      Q6=Z**I
      Q7=Q2+Q3+Q6/(FACT+Q4+Q5)
      Q=Q-Q7
      IF (ABS(Q7).LT..0001) GO TO 40
30      CONTINUE
40      X1=1.0-(B*D)
      X2=B
      X3=-G
      CALL GAMMA(X1,G1)
      CALL GAMMA(X2,G2)
      CALL GAMMA(X3,G3)
      Q8=1.0/(B*B*D)
      Q9=1.0-(K/(D-1.0))
      R1=Z**(B*D)
      R2=Q8+Q9+G1+G2+R1/G3
      R3=(1.0+K)/(B*D*(2.0-ALPHA))
      R4=Q1+(K*(1.0+Q1))
      R5=(1.0-ALPHA)*X1
      R6=R4+Z/R5
      R7=(Z+Z*(1.0-G)+(Q1+(K*(2.0+Q1))))/(ALPHA+B*D*(1.+X1))
      Q=Q-R2-R3+R6
      IF (ALPHA.LT.0.) Q=Q-R7
      TYPE 11,Q
11      FORMAT(10X,F10.5)
      RETURN
      END

```

C
C "HX" IS A SUBROUTINE THAT CALCULATES H(X).

```

SUBROUTINE HX(B,D,C,Z,H)
REAL B,D,C,Z,G,X1,X2,X3,G1,G2,G3,GTERM,CTERM,ZTERM
1,F1,F2,F3,CONST,F(2),NTERM,E,H
INTEGER FACT,N,L,M
G=B*(D-1.0)
E=.0001
IF (Z.LT.-1.) GO TO 40
X1=1.0-(B*D)
X2=B
X3=-G
CALL GAMMA(X1,G1)
CALL GAMMA(X2,G2)
CALL GAMMA(X3,G3)
GTERM=G1+G2/G3
CTERM=1.-(C/(D-1.))
ZTERM=Z*(ABS(Z)**((B*D)-1.))
F1=-G
F2=-B*D

```

```

C
F3=1.0-(B+D)
DO 30 N=1,2
CONST=F1+F2/F3
F(N)=1.0+(CONST+Z)
FACT=1
DO 10 L=2,100
FACT=FACT*L
M=L-1
CONST=CONST*(F1+M)*(F2+M)/(F3+M)
NTERM=CONST*(Z**L)/FACT
F(N)=F(N)+NTERM
IF (NTERM.LT.E) GO TO 20
10 CONTINUE
20 IF (N.LT.2) F1=F1+1.0
30 CONTINUE
H=(CTERM+GTERM+ZTERM)+F(1)+(C+F(2))
GO TO 90
40 X1=-1.0-B
X2=-B
CALL GAMMA(X1,G1)
CALL GAMMA(X2,G2)
GTERM=D+B+C*G1/G2
ZTERM=(-Z)**G
F1=-G
F2=B
F3=1.0+B
DO 70 N=1,2
CONST=F1+F2/F3
F(N)=1.0+(CONST/Z)
FACT=1
DO 50 L=2,100
FACT=FACT*L
M=L-1
CONST=CONST*(F1+M)*(F2+M)/(F3+M)
NTERM=CONST*((1./Z)**L)/FACT
F(N)=F(N)+NTERM
IF (NTERM.LT.E) GO TO 60
50 CONTINUE
60 IF (N.EQ.2) GO TO 80
F1=F1+1.0
F2=F2+1.0
F3=F3+1.0
70 CONTINUE
80 H=(D+ZTERM+F(1))-(GTERM+(ZTERM/(-Z))*F(2))
90 RETURN
END

```

THE CONCEPT OF THE PSEUDOSPINODAL
IN CRITICAL PHENOMENA

by

JUNAIDAH OSMAN

B.S., Northern Illinois University, 1978

AN ABSTRACT OF A MASTER'S THESIS

submitted in partial fulfillment of the

requirements for the degree

MASTER OF SCIENCE

Department of Physics

KANSAS STATE UNIVERSITY
Manhattan, Kansas

1981

ABSTRACT

Benedek's pseudospinodal assumption is revised by adding an extra term. This extra term is suggested by the form of the pseudospinodal assumption for the spherical model. The equation of state derived from this assumption provides a good representation of the universality classes (3,1), (3,2) and (3,3); the equation compares well with other equations for these systems. From the revised assumption and the equation of state, expressions for the universal amplitude ratios are also derived. Agreement with data and other theoretical predictions for these classes of systems is obtained.

Using all available experimental evidence, the possible existence of a universal pseudospinodal for the universality class (3,1) is shown.

These results support the usefulness of the pseudospinodal concept in critical phenomena--a concept that has been argued by some theoretical considerations.